École Polytechnique Fédérale de Lausanne

Master Thesis

Accelerated Sensor Fusion for Drones and a Simulation Framework for Spatial

Author

Ruben Fiszel $ruben. fiszel@epfl.\,ch$

Supervisors

 $\begin{array}{l} {\rm Prof.\ Martin\ Odersky} \\ {\rm LAMP} \mid {\rm EPFL} \\ {\it martin.odersky@epfl.ch} \end{array}$

August 29, 2017

Prof. Oyekunle A. Olukotun PPL | Stanford kunle@stanford.edu





Abstract

We present here a novel asynchronous Rao-Blackwellized Particle Filter for POSE estimation of drones and its implementation on hardware with the spatial language. We also present contributions to the spatial language under the form of development tools: scala-flow, a prototyping data-flow tool inspired by Simulink with a spatial integration. Finally, as a required component of scala-flow's spatial integration, an interpreter for the spatial language was also developed.

Contents

Ta	able of Contents	2
In	troduction	3
	Moore's law end	3
	The rise of Hardware	3
	Hardware as companion accelerators	5
	The right metric: Perf/Watt	5
	Spatial	5
	Embedded systems and drones	6
1	Sensor fusion algorithm for POSE estimation of drones: Asyn-	
	chronous Rao-Blackwellized Particle filter	7
	Drones and collision avoidance	8
	Sensor fusion	8
	Notes on notation and conventions	9
	POSE	10
	Data generation	10
	Quaternion	11
	Helper functions and matrices	12
	Model	13
	Sensors	13
	Control inputs	17
	Model dynamic	17
	State	17
	Observation	18
	Filtering and smoothing	18
	Complementary Filter	18
	Asynchronous Augmented Complementary Filter	21
	Kalman Filter	22
	Asynchronous Kalman Filter	24
	Extended Kalman Filters	24
	Unscented Kalman Filters	28
	Particle Filter	30
	Rac Blackwellized Particle Filter	34

	Algorithm summary	38
	Results	40
	Conclusion	41
2	A simulation tool for data flows with spatial integration: scala-	
	flow	44
	Purpose	44
	Source, Sink and Transformations	45
	Demo	46
	Block	48
	Buffer and cycles	49
	Source API	49
	Batch	52
	Scheduling	52
	Replay	53
	Graph construction	53
	Spatial integration	54
	Conclusion	54
3	An interpreter for spatial	55
-	Spatial: An Hardware Description Language	
	Spatial: An Hardware Description Language	55
	Argon	55 56
	Argon	55
	Argon	55 56 56
	Argon	55 56 56 56 57
4	Argon	55 56 56 56 57
	Argon	55 56 56 56 57 58
	Argon	55 56 56 56 57 58 58
	Argon	55 56 56 56 57 58 58 58
	Argon	55 56 56 56 57 58 58
4	Argon	55 56 56 56 57 58 58 58
4 Co	Argon Simulation in Spatial Benefits of the interpreter Interpreter Spatial implementation of an asynchronous Rao-Blackwellized Particle Filter A matrix library as stdlib Mini Particle Filter Rao Blackwellized Particle Filter	55 56 56 56 57 58 58 58 58

Introduction

Moore's law end

The Moore's law¹ has prevailed in the computation world for the last 4 decades. With each generation of processor, the promise of an exponentially faster execution. Transistors are reaching the scale of 10nm, only 100 times bigger than an atom. Unfortunately, the quantum rules of physics which govern the infinitesimally, start to manifest themselves. In particular, quantum tunneling move electrons from classically insurmountable barrier, making computations approximate, containing a non negligible fraction of errors.

The rise of Hardware

Hardware and Software designate here respectively programs that are executed as code for a general purpose processing unit and programs that are synthesized as circuits. The dichotomy is not very well-defined and we can think of it as a spectrum. General-purpose computing on graphics processing units (GPGPU) is in-between in the sense that it is general purpose but relevant only for embarrassingly parallel tasks² and very efficient when used well. They have benefited from high-investment and many generations of iterations and hence, for some tasks, can rivalize or even surpass Hardware.

Hardware has always been there but application-specific integrated circuit (ASIC) has prohibitive costs upfront (in the range of \$100M for a tapeout). Reprogrammable hardware like field-programmable gate array (FPGA) have only been used marginally and for some specific industries like high-frequency trading. But now Hardware is the next natural step to increase performance,

¹The observation that the number of transistors in a dense integrated circuit doubles approximately every two years.

²An embarrassingly parallel task is one where little or no effort is needed to separate the problem into a number of parallel tasks. This is often the case where there is little or no dependency or need for communication between those parallel tasks, or for results between them.

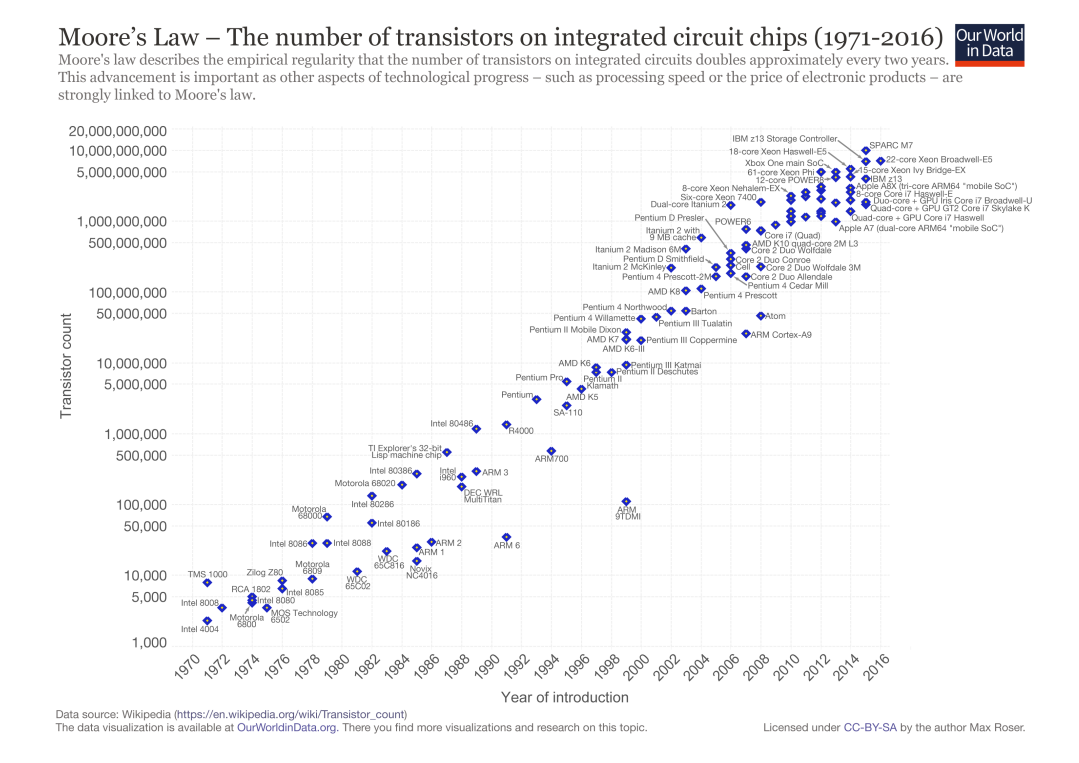
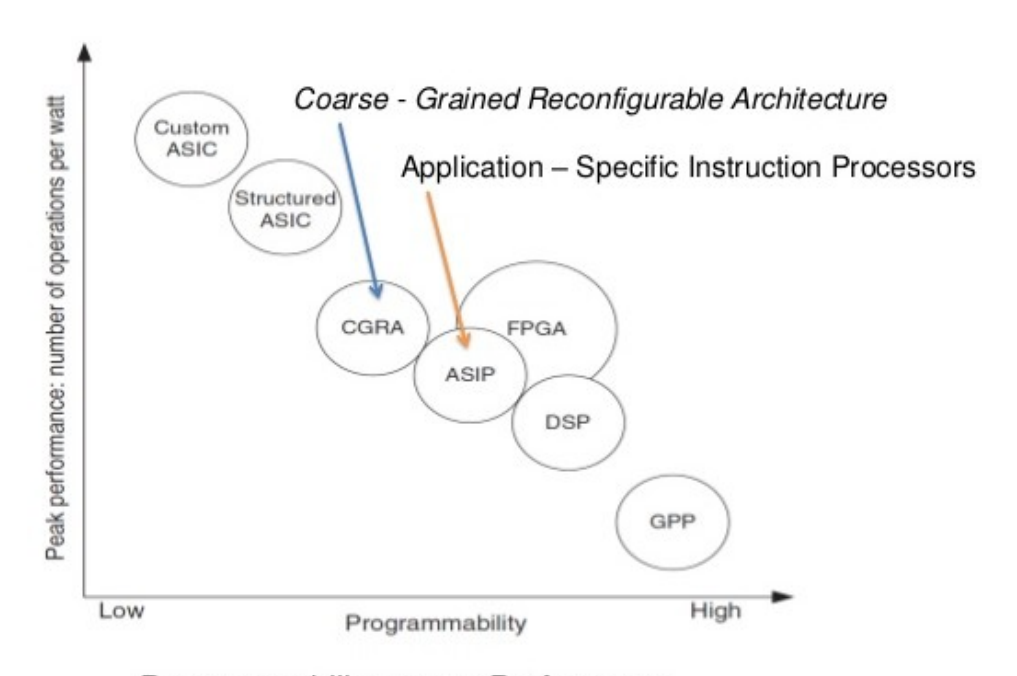


Figure 1: The number of transistors throughout the years. We can observe a recent start of a decline



Programmability versus Performance

Figure 2: Hardware vs Software

at least until a computing revolution happen, like quantum computing, but this is not realist for the near future. However, hardware do not enjoy the same quality of tooling, language and integrated development environments (IDE) as software. This is one the motivation behind Spatial: bridging the gap between Software and Hardware by abstracting control flows through language constructions.

Hardware as companion accelerators

In most case, hardware would be inappropriate: running an OS as hardware would be impracticable. Nevertheless, as a companion to a central-processing unit (CPU also called "the host"), it is possible to get the best of both world. The flexibility of software on a CPU with the speed of hardware. In this setup, hardware is considered an "accelerator" (Hence, the term "accelerating hardware"). It accelerates the most demanding subroutines of the CPU. This companionship is already present in modern computer desktops under the form of GPUs for *shader* operations and sound card for complex sound transformation/output.

The right metric: Perf/Watt

The right metric for accelerator is performance by energy, as measured in FLOPS per Watt. This is a fair metric for the comparison of different hardware and architecture because it reveals its intrinsic properties as a computing element.. If the metric was solely performance, then it would suffice to stack the same hardware and eventually a reach the scale of a super-computer. Perf per dollar is not a good metric either because you should also account for the cost of energy at runtime. Hence, Perf/Watt seems like a fair metric to compare architectures.

Spatial

At the dawn lab, under the lead of Prof. Kunle and his grad students, is developed a scala DSL spatial and its compiler to program Hardware in a higher-level, more user-friendly, more productive language than Verilog. In particular, the control flows are automatically generated when possible. This should enable software engineers to unlock the potential of Hardware. A custom CGRA, Plasticine, has been developed in parallel to Spatial. It leverages some recurrent patterns: the parallel patterns and aims to be the most efficient reprogrammable architecture for Spatial.

There is a large upfront cost but once at a big enough scale, Plasticine

could be deployed as an accelerator in a wide range of use-cases, from the most demanding server applications to embedded systems with heavy computing requirements.

Embedded systems and drones

Embedded systems are limited by the amount of power at disposal from the battery and might also have size constraints. At the same time, especially for autonomous vehicles, there is a great need for computing power.

Thus, developing drone applications with spatial demonstrates the advantages of the platform. As a matter of fact, the filter implementation was only made possible because it is run on an accelerating hardware. It would be unfeasible to run it on more conventional micro-transistors. This is why the family in which belong the filter developed here, particles filters, being very computationally expensive, are very seldom used for drones.

1 | Sensor fusion algorithm for POSE estimation of drones: Asynchronous Rao-Blackwellized Particle filter

POSE is the combination of the position and orientation of an object. POSE estimation is important for drones. Indeed, It is a subroutine of SLAM (Simultaneous localization and mapping) and it is a central part of motion planning and motion control. More accurate and more reliable POSE estimation results in more agile, more reactive and safer drones. Drones are an intellectually stimulating subject but in the near-future they might also see their usage increase exponentially. In this context, developing and implementing new filter for POSE estimation is both important for the field of robotics but also to demonstrate the importance of hardware acceleration. Indeed, the best and last filter presented here is only made possible because it can be hardware accelerated with Spatial. However, the spatial implementation will be presented in Part III.

Before expanding on the Rao-Blackwellized particle filter, we will introduce here several other filters for POSE estimation for highly dynamic objects: Complementary filter, Kalman Filter, Extended Kalman Filter, Particle Filter and finally Rao-Blackwellized Particle filter. The order is from the most conceptually simple, to the most complex. This order is justified because complex filters aim to alleviate some of the flaws of their simpler counterpart. It is important to understand which one and how.

All the following filters are developed and tested in scala-flow. scala-flow will be expanded in part 2 of this thesis. For now, we will focus on the model and the results, and leave the implementation details for later.

Drones and collision avoidance

The original motivation for the development of accelerated POSE estimation is for the task of collision avoidance by quadcopters. In particular, a collision avoidance algorithm developed at the ASL lab and demonstrated here (https://youtu.be/kdlhfMiWVV0)



Figure 1.1: Ross Allen fencing with his drone

where the drone avoids the sword attack from its creator. At first, it was thought of accelerating the whole algorithm but it was found that one of the most demanding subroutine was pose estimation. Moreover, it was wished to increase the processing rate of the filter such that it could match the input with the fastest sampling rate: its inertial measurement unit (IMU) containing an accelerometer, a gyroscope and a magnetometer.

The flamewheel f450 is the typical drone in this category. It is surprisingly fast and agile. Given the proper command, it can generate enough thrust to avoid in a very short lapse of time any incoming object.

Sensor fusion

Sensor fusion is the combination of sensory data or data derived from disparate sources such that the resulting information has less uncertainty than would be possible if these sources were to be used individually. In the context of drones, it is very useful because it enables to combine many unprecise sensor measurement to form a more precise one like having precise positionning from 2 less precise GPS (dual GPS setting). It can also permit to combine sensors with different sampling rates: typically precise sensors with low sampling rate and less precise sensors with high sampling rate. Both cases are gonna be relevant here.



Figure 1.2: The Flamewheel f450

A fundamental explanation why this is possible comes from the central limit theorem: one sample from a distribution with a low variance is as good as n sample from a distribution with variance n times higher.

$$\mathbb{V}(X_i) = \sigma^2 \qquad \mathbb{E}(X_i) = \mu$$
$$\bar{X} = \frac{1}{n} \sum X_i$$
$$\mathbb{V}(\bar{X}) = \frac{\sigma^2}{n} \qquad \mathbb{E}(\bar{X}) = \mu$$

Notes on notation and conventions

The referential by default is the fixed world frame.

- \bullet **x** designates a vector
- x_t is the random variable x at time t
- $x_{t1:t2}$ is the product of the random variable x between t1 included and t2 included
- $x^{(i)}$ designates the random variable x of the arbitrary particle i
- \hat{x} designates an estimated variable

POSE

POSE is the task of estimating the position and orientation of an object through time. It is a subroutine of Software Localization And Mapping (SLAM). We can formelize the problem as:

At each timestep, find the best expectation of a function of the hidden variable state (position and orientation), from their initial distribution and the history of observable random variables (such as sensor measurements).

- The state \mathbf{x}
- The function $g(\mathbf{x})$ such that $g(\mathbf{x}_t) = (\mathbf{p}_t, \mathbf{q}_t)$ where \mathbf{p} is the position and \mathbf{q} is the attitude as a quaternion.
- The observable variable ${\bf y}$ composed of the sensor measurements ${\bf z}$ and the control input ${\bf u}$

The algorithm inputs are:

- control inputs \mathbf{u}_t (the commands sent to the flight controller)
- sensor measurements \mathbf{z}_t coming from different sensors with different sampling rate
- information about the sensors (sensor measurements biases and matrix of covariance)

Data generation

The difficulties with using real flight data is that you need to get the *true* trajectory and that you need enough data to check the efficiency of the filters.

To avoid those issues, the flight data is simulated through a model of trajectory generation from [1]. Data generated this way are called synthetic data. The algorithm input are the motion primitives defined by the quad-copter's initial state, the desired motion duration, and any combination of components of the quadcopter's position, velocity and acceleration at the motion's end. The algorithm is essentially a closed form solution for the given primitives. The closed form solution minimizes a cost function related to the input aggressiveness.

The bulk of the method is that a differential equation representing the difference of position, velocity and acceleration between the starting and ending state is solved with the Pontryagin's minimum principle using the appropriate Hamiltonian. Then, from that closed form solution, a per-axis cost can be calculated to pick the "least aggressive" trajectory out of different candidates. Finally, the feasibility of the trajectory is computed using the constraints of maximum thrust and body rate (angular velocity) limits. For the purpose of this work, a scala implementation of the model was realized. Then, some keypoints containing Gaussian components for the position, velocity acceleration, and duration were tried until a feasible set of keypoints was found. This method of data generation is both fast and a good enough approximation of the actual trajectories that a drone would perform in the real world.

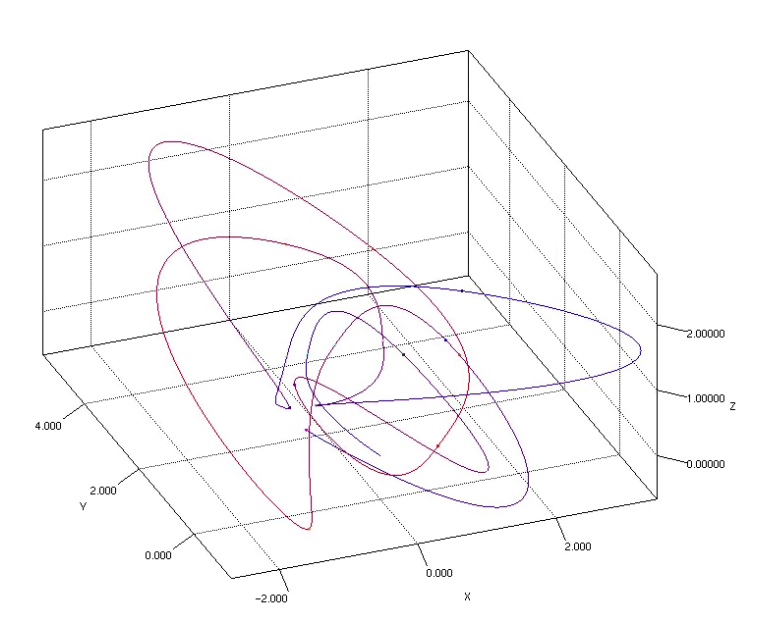


Figure 1.3: Visualization of an example of a synthetic generated flight trajectory

Quaternion

Quaternions are extensions of complex numbers with 3 imaginary parts. Unit quaternions can be used to represent orientation, also referred to as attitude. Quaternions algebra make rotation composition simple and quaternions avoid the issue of gimbal lock.¹ In all filters presented, quaternions represent the attitude.

$$\mathbf{q} = (q.r, q.i, q.j, q.k)^t = (q.r, \boldsymbol{\varrho})^T$$

Quaternion rotations composition is: q_2q_1 which results in q_1 being

¹Gimbal lock is the loss of one degree of freedom in a three-dimensional, three-gimbal mechanism that occurs when the axes of two of the three gimbals are driven into a parallel configuration, "locking" the system into rotation in a degenerate two-dimensional space.

rotated by the rotation represented by q_2 . From this, we can deduce that angular velocity integrated over time is simply q^t if q is the local quaternion rotation by unit of time. The product of two quaternions (also called Hamilton product) is computable by regrouping the same type of imaginary and real components together and accordingly to the identity:

$$i^2 = j^2 = k^2 = ijk = -1$$

Rotation of a vector by a quaternion is done by: qvq^* where q is the quaternion representing the rotation, q^* its conjugate and v the vector to be rotated. The conjugate of a quaternion is:

$$q^* = -\frac{1}{2}(q + iqi + jqj + kqk)$$

The distance of between two quaternions, useful as an error metric is defined by the squared Frobenius norms of attitude matrix differences [2].

$$||A(\mathbf{q}_1) - A(\mathbf{q}_2)||_F^2 = 6 - 2Tr[A(\mathbf{q}_1)A^t(\mathbf{q}_2)]$$

where

$$A(\mathbf{q}) = (q.r^2 - \|\boldsymbol{\varrho}\|^2)I_{3\times 3} + 2\boldsymbol{\varrho}\boldsymbol{\varrho}^T - 2q.r[\boldsymbol{\varrho}\times]$$

$$[\boldsymbol{\varrho} \times] = \left(\begin{array}{ccc} 0 & -q.k & q.j \\ q.k & 0 & -q.i \\ -q.j & q.i & 0 \end{array} \right)$$

Helper functions and matrices

We introduce some helper matrices.

- $\mathbf{R}_{b2f}\{\mathbf{q}\}$ is the body to fixed vector rotation matrix. It transforms vector in the body frame to the fixed world frame. It takes as parameter the attitude \mathbf{q} .
- $\mathbf{R}_{f2b}\{\mathbf{q}\}$ is its inverse matrix (from fixed to body).
- $\mathbf{T}_{2a} = (0, 0, 1/m)^T$ is the scaling from thrust to acceleration (by dividing by the weight of the drone: $\mathbf{F} = m\mathbf{a} \Rightarrow \mathbf{a} = \mathbf{F}/m$) and then multiplying by a unit vector (0, 0, 1)

$$R2Q(\boldsymbol{\theta}) = (\cos(\|\boldsymbol{\theta}\|/2), \sin(\|\boldsymbol{\theta}\|/2) \frac{\boldsymbol{\theta}}{\|\boldsymbol{\theta}\|})$$

is a function that convert from a local rotation vector $\boldsymbol{\theta}$ to a local quaternion rotation. The definition of this function come from converting $\boldsymbol{\theta}$ to a body-axis angle, and then to a quaternion.

$$Q2R(\mathbf{q}) = (q.i * s, q.j * s, q.k * s)$$

is its inverse function where $n = \arccos(q.w) * 2$ and $s = n/\sin(n/2)$

• Δt is the lapse of time between t and the next tick (t+1)

Model

The drone is assumed to have rigid-body physics. It is submitted to the gravity and its own inertia. A rigid body is a solid body in which deformation is zero or so small it can be neglected. The distance between any two given points on a rigid body remains constant in time regardless of external forces exerted on it. This enable to summarize the forces from the rotor as a thrust oriented in the direction normal to the plane formed by the 4 rotors, and an angular velocity.

Those variables are sufficient to describe the evolution of our drone with rigid-body physics:

- a the total acceleration in the fixed world frame
- v the velocity in the fixed world frame
- **p** the position in the fixed world frame
- ω the angular velocity
- q the attitude in the fixed world frame

Sensors

The sensors at disposition are:

• Accelerometer: It generates $\mathbf{a_A}$ a measurement of the total acceleration in the body frame referential the drone is submitted to at a **high** sampling rate. If the object is submitted to no acceleration then the accelerometer measure the earth's gravity field from. From that information, it could be possible to retrieve the attitude. Unfortunately, we are in a highly dynamic setting. Thus, it is possible when we can subtract the drone's acceleration from the thrust to the total acceleration. This would require to know exactly the force exerted by the rotors at each instant. In this work, we assume that doing that separation, while being theoretically possible, is too impractical. The measurements model is:

$$\mathbf{a}_{\mathbf{A}}(t) = \mathbf{R}_{f2b}\{\mathbf{q}(t)\}\mathbf{a}(t) + \mathbf{a}_{\mathbf{A}}^{\epsilon}$$

where the covariance matrix of the noise of the accelerometer is $\mathbf{R_{a_{A\,3\times3}}}$ and

$$\mathbf{a_A}^{\epsilon} \sim \mathcal{N}(\mathbf{0}, \mathbf{R_{a_A}})$$

•

• Gyroscope:It generates $\omega_{\mathbf{G}}$ a measurement of the angular velocity in the body frame of the drone at the last timestep at a **high** sampling rate. The measurement model is:

$$\omega_{\mathbf{G}}(t) = \omega + \omega_{\mathbf{G}}^{\epsilon}$$

where the covariance matrix of the noise of the accelerometer is $\mathbf{R}_{\omega_{\mathbf{G}} 3 \times 3}$ and

$$oldsymbol{\omega_{G_t}}^\epsilon \sim \mathcal{N}(\mathbf{0}, \mathbf{R}_{oldsymbol{\omega_G}})$$

•

Position: It generates p_V a measurement of the current position at a low sampling rate. This is usually provided by a Vicon (for indoor), GPS, a Tango or any other position sensor. The measurement model is:

$$\mathbf{p}_{\mathbf{V}}(t) = \mathbf{p}(t) + \mathbf{p}_{\mathbf{V}}^{\epsilon}$$

where the covariance matrix of the noise of the position is $\mathbf{R}_{\mathbf{p}_{\mathbf{V}3\times3}}$ and

$$\mathbf{p_V}^\epsilon \sim \mathcal{N}(\mathbf{0}, \mathbf{R_{p_V}})$$

.

• Attitude: It generates $\mathbf{q_V}$ a measurement of the current attitute. This is usually provided in addition to the position by a **Vicon** or a **Tango** at a **low** sampling rate or the **Magnemoter** at a **high** sampling rate if the environment permit it (no high magnetic interference nearby like iron contamination). The magnetometer retrieves the attitude by assuming that the sensed magnetic field corresponds to the earth's magnetic field. The measurement model is:

$$\mathbf{q}_{\mathbf{V}}(t) = \mathbf{q}(t) * R2Q(\mathbf{q}_{\mathbf{V}}^{\epsilon})$$

where the 3×3 covariance matrix of the noise of the attitude in radian before being converted by R2Q is $\mathbf{R}_{\mathbf{q_{V3}}\times 3}$ and

$$\mathbf{q_V}^\epsilon \sim \mathcal{N}(\mathbf{0}, \mathbf{R_{q_V}})$$

.

• Optical Flow: A camera that keeps track of the movement by comparing the difference of the position of some reference points. By using a companion distance sensor, it is able to retrieve the difference between the two perspective and thus the change in angle and position.

$$\mathbf{dq_O}(t) = (\mathbf{q}(t-k)\mathbf{q}(t)) * R2Q(\mathbf{dq_O}^{\epsilon})$$

$$\mathbf{dp_O}(t) = (\mathbf{p}(t) - \mathbf{p}(t-k)) + \mathbf{dp_O}^{\epsilon}$$

where the 3×3 covariance matrix of the noise of the attitude variation in radian before being converted by R2Q is $\mathbf{R_{dqo}}_{3\times3}$ and

$$\mathbf{dq_O}^\epsilon \sim \mathcal{N}(\mathbf{0}, \mathbf{R_{dq_O}})$$

and the position variation covariance matrix $\mathbf{R_{dpo}}_{3\times3}$ and

$$\mathbf{dp_O}^\epsilon \sim \mathcal{N}(\mathbf{0}, \mathbf{R_{dp_O}})$$

Figure 1.4: Optical flow from a moving drone

The notable difference with the position or attitude sensor is that the optical flow sensor, like the IMU, only captures time variation, not absolute values.

• Altimeter: An altimeter is a sensor that measure the altitude of the drone. For instance a LIDAR measure the time for the laser wave to reflect on a surface that is assumed to be the ground. A smart strategy is to only use the altimeter is oriented with a low angle to the earth, else you also have to account that angle in the estimation of the altitude.

$$z_A(t) = \sin(\operatorname{pitch}(\mathbf{q}(\mathbf{t})))(\mathbf{p}(t).z + z_A^{\epsilon})$$

 $R_{z_A3\times3}$ and

$$z_A^{\epsilon} \sim \mathcal{N}(0, R_{z_A})$$

Some sensors are more relevant indoor and some others outdoor:



Figure 1.5: Rendering of the LIDAR laser of an altimeter

• Indoor: The sensors available indoor are the accelerometer, the gyroscope and the Vicon. The Vicon is a system composed of many sensors around a room that is able to track very accurately the position and orientation a mobile object. One issue with relying solely on the Vicon is that the sampling rate is low.

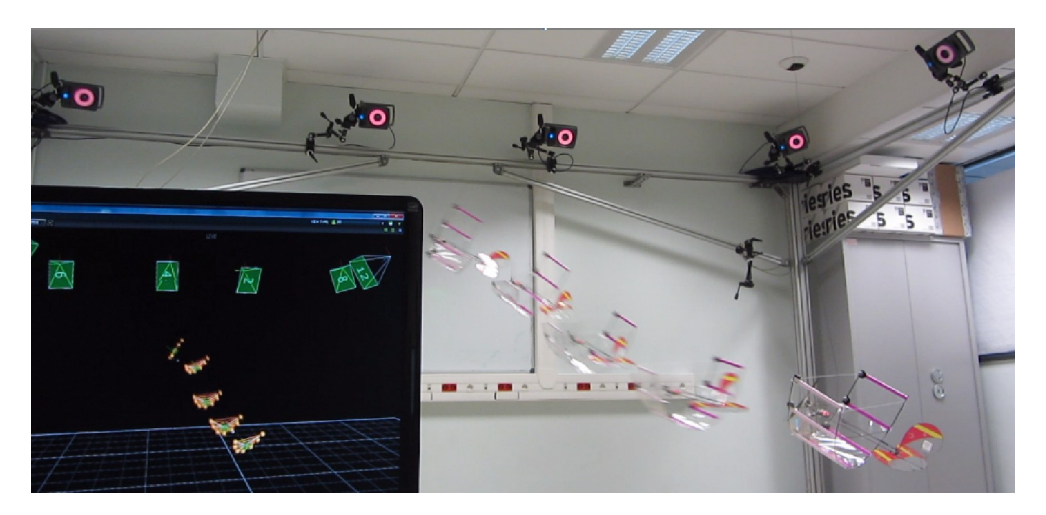


Figure 1.6: A Vicon setup

• Outdoor: The sensors available outdoor are the accelerometer, the gyroscope, the magnetometer, two GPS, an optical flow and an altimeter.

We assume that since the biases of the sensor could be known prior to the flight, the sensor have been calibrated and output measurements with no bias. Some filters like the ekf2 of the px4 flight stack keep track of the sensor biases but this is a state augmentation that was not deemed worthwhile.

Control inputs

Observations from the control input are not strictly speaking measurements but input of the state-transition model. The IMU is a sensor, thus strictly speaking, its measurements are not control inputs. However, in the literature, it is standard to use its measurements as control inputs. One of the advantage is that the accelerometer measures acceleration and angular velocity, raw values close from the input we need in our state-transition. If we used a transformation of the thrust sent as command to the rotors, we would have to account for the rotors imprecision, the wind and other disturbances. Another advantage is that since the IMU has very high sampling rate, we can update very frequently the state with new transitions. The drawback is that the accelerometer is noisy. Fortunately, we can take into account the noise as a process model noise.

The control inputs at disposition are:

- Acceleration: $\mathbf{a}_{\mathbf{A}t}$ from the acceleremeter
- Angular velocity: $\omega_{\mathbf{G}t}$ from the gyroscope.

Model dynamic

```
• \mathbf{a}(t+1) = \mathbf{R}_{b2f}\{\mathbf{q}(t+1)\}(\mathbf{a}_{\mathbf{A}t} + \mathbf{a}_{\mathbf{A}t}^{\epsilon}) \text{ where } \mathbf{a}_{t}^{\epsilon} \sim \mathcal{N}(\mathbf{0}, \mathbf{Q}_{\mathbf{a}t})
• \mathbf{v}(t+1) = \mathbf{v}(t) + \Delta t \mathbf{a}(t) + \mathbf{v}_{t}^{\epsilon} \text{ where } \mathbf{v}_{t}^{\epsilon} \sim \mathcal{N}(\mathbf{0}, \mathbf{Q}_{\mathbf{v}_{t}})
• \mathbf{p}(t+1) = \mathbf{p}(t) + \Delta t \mathbf{v}(t) + \mathbf{p}_{t}^{\epsilon} \text{ where } \mathbf{p}_{t}^{\epsilon} \sim \mathcal{N}(\mathbf{0}, \mathbf{Q}_{\mathbf{p}_{t}})
• \boldsymbol{\omega}(t+1) = \boldsymbol{\omega}_{\mathbf{G}t} + \boldsymbol{\omega}_{\mathbf{G}t}^{\epsilon} \text{ where } \mathbf{p}_{t}^{\epsilon} \sim \mathcal{N}(\mathbf{0}, \mathbf{Q}_{\mathbf{\omega}_{\mathbf{G}t}})
```

• $\mathbf{q}(t+1) = \mathbf{q}(t) * R2Q(\Delta t \boldsymbol{\omega}(t))$

Note that in our model, $\mathbf{q}(t+1)$ must be known. Fortunately, as we will see later, our Rao-Blackwellized Particle Filter is conditionned under the attitude so it is known.

State

The time series of the variables of our dynamic model constitute a hidden markov chain. Indeed, the model is "memoryless" and depends only on the current state and a sampled transition.

States contain variables that enable us to keep track of some of those hidden variables which is our ultimate goal (for POSE \mathbf{p} and \mathbf{q}). States at time t are denoted by \mathbf{x}_t . Different filters require different state variables depending on their structure and assumptions.

Observation

Observations are revealed variables conditioned under the variables of our dynamic model. Our ultimate goal is to deduce the states from the observations.

Observations contain the control input ${\bf u}$ and the measurements ${\bf z}$.

$$\mathbf{y}_t = (\mathbf{z}_t, \mathbf{u}_t)^T = (\mathbf{p}_{\mathbf{V}_t}, \mathbf{q}_{\mathbf{V}_t}), (t_{Ct}, \boldsymbol{\omega}_{\mathbf{C}_t}))^T$$

Filtering and smoothing

Smoothing is the statistical task of finding the expectation of the state variable from the past history of observations and multiple observation variables ahead

$$\mathbb{E}[q(\mathbf{x}_{0:t})|\mathbf{y}_{1:t+k}]$$

Which expand to,

$$\mathbb{E}[(\mathbf{p}_{0:t},\mathbf{q}_{0:t})|(\mathbf{z}_{1:t+k},\mathbf{u}_{1:t+k})]$$

k is a contant and the first observation is y_1

Filtering is a kind of smoothing where you only have at disposal the current observation variable (k = 0)

Complementary Filter

The complementary filter is the simplest of all filter and commonly used to retrieve the attitude because of its low computational complexity. The gyroscope and accelerometer both provide a measurement that can help us to estimate the attitude. Indeed, the gyroscope reads noisy measurement of the angular velocity from which we can retrieve the new attitude from the past one by time integration: $\mathbf{q}_t = \mathbf{q}_{t-1} * R2Q(\Delta t\omega)$.

This is commonly called "Dead reckoning" 2 and is prone to accumula-

²The etymology for "Dead reckoning" comes from the mariners of the XVIIth century that used to calculate the position of the vessel with log book. The interpretation of "dead" is subject to debate. Some argue that it is a misspelling of "ded" as in "deduced". Others argue that it should be read by its old meaning: *absolute*.

tion error, referred as drift. Indeed, like Brownian motions, even if the process is unbiased, the variance grows with time. Reducing the noise cannot solve the issue entirely: even with extremely precise instruments, you are subject to floating-point errors.

Fortunately, even though the accelerometer gives us a highly noisy (vibrations, wind, etc ...) measurement of the orientation, it is not subject to drift because it does not rely on accumulation. Indeed, if not subject to other accelerations, the accelerometer measures the gravity field orientation. Since this field is oriented toward earth, it is possible to retrieve the current rotation from that field and by extension the attitude. However, in the case of a drone, it is subject to continuous and significant acceleration and vibration. Hence, the assumption that we retrieve the gravity field directly is wrong. Nevertheless, We could solve this by subtracting the acceleration deduced from the thrust control input. It is unpractical so this approach is not pursued in this work, but understanding this filter is still useful.

The idea of the filter itself is to combine the precise "short-term" measurements of the gyroscope subject to drift with the "long-term" measurements of the accelerometer.

State

This filter is very simple and it is only needed to store as a state the last estimated attitude along with its timestamp (to calculate Δt).

$$\mathbf{x}_t = \mathbf{q}_t$$

$$\hat{\mathbf{q}}_{t+1} = \alpha(\hat{\mathbf{q}}_t + \Delta t \omega_t) + (1 - \alpha)\mathbf{q}_{\mathbf{A}_{t+1}}$$

 $\alpha \in [0,1]$. Usually, α is set to a high-value like 0.98. It is very intuitive to see why this should approximately "work", the data from the accelerometer continuously correct the drift from the gyroscope.

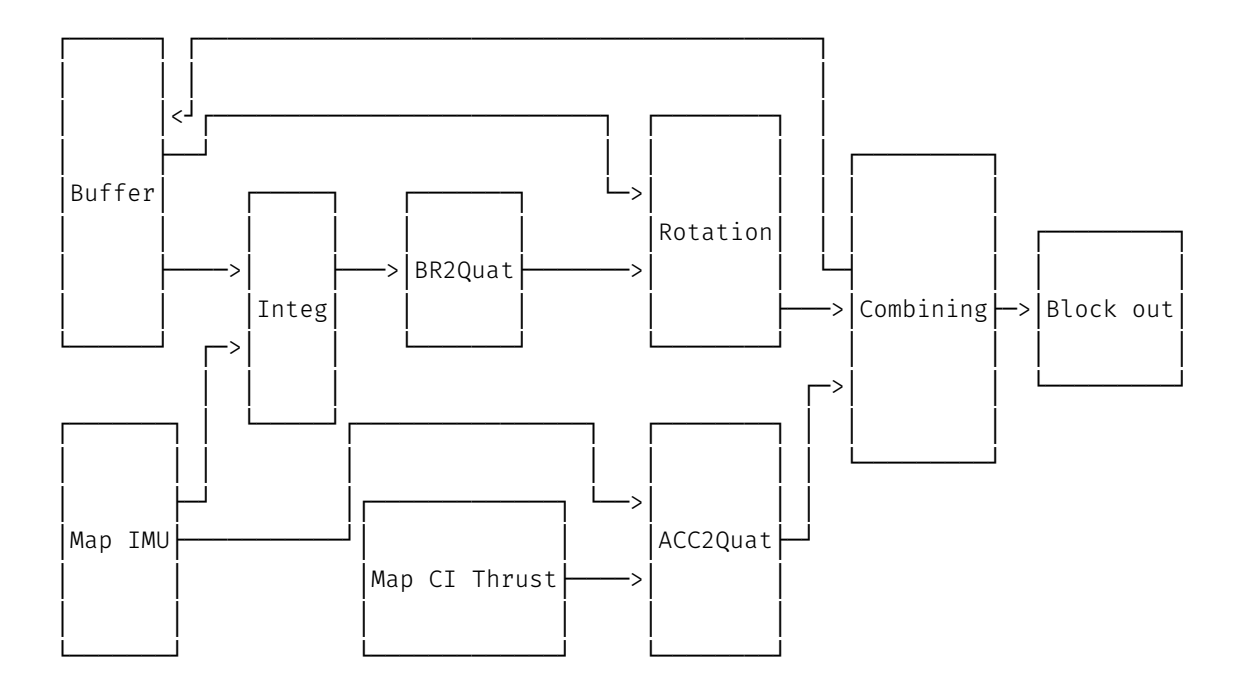


Figure 1.7: Complementary Filter graph structure

Figure 9 is the plot of the distance from the true quaternion after 15s of an arbitrary trajectory when $\alpha=1.0$ meaning that the accelerometer does not correct the drift.

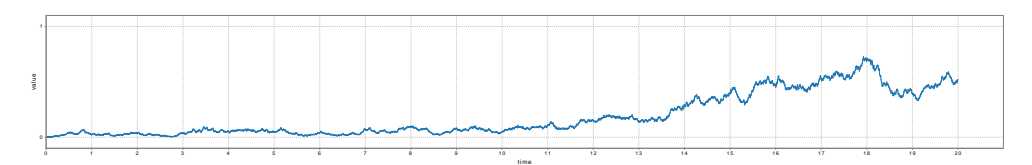


Figure 1.8: CF with alpha = 1.0

Figure 10 is that same trajectory with $\alpha = 0.98$.

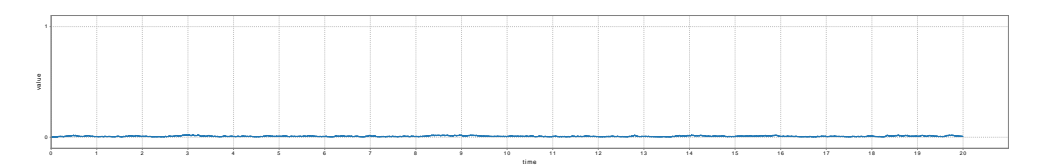


Figure 1.9: CF with alpha = 0.98

We can observe here the long-term importance of being able to correct the drift, even if ever so slightly at each timestep.

Asynchronous Augmented Complementary Filter

As explained previously, in this highly-dynamic setting, combining the gyroscope and the accelerometer to retrieve the attitude is not satisfactory. However, we can reuse the intuition from the complementary filter, which is to combine precise but drifting short-term measurements to other measurements that do not suffer from drift. This enable a simple and computationally inexpensive novel filter that we will be able to use later as a baseline. In this case, the short-term measurements are the acceleration and angular velocity from the IMU, and the non drifting measurements come from the Vicon.

We will also add the property that the data from the sensors are asynchronous. As with all following filters, we deal with asynchronicity by updating the state to the most likely state so far for any new sensor measurement incoming. This is a consequence of the sensors having different sampling rate.

• IMU update

$$\mathbf{v}_{t} = \mathbf{v}_{t-1} + \Delta t_{v} \mathbf{a}_{At}$$

$$\boldsymbol{\omega}_{t} = \boldsymbol{\omega}_{Gt}$$

$$\mathbf{p}_{t} = \mathbf{p}_{t-1} + \Delta t \mathbf{v}_{t-1}$$

$$\mathbf{q}_{t} = \mathbf{q}_{t-1} R2Q(\Delta t \boldsymbol{\omega}_{t-1})$$

• Vicon update

$$\mathbf{p}_{t} = \alpha \mathbf{p}_{\mathbf{V}} + (1 - \alpha)(\mathbf{p}_{t-1} + \Delta t \mathbf{v}_{t-1})$$
$$\mathbf{q}_{t} = \alpha \mathbf{q}_{\mathbf{V}} + (1 - \alpha)(\mathbf{q}_{t-1} R2Q(\Delta t \boldsymbol{\omega}_{t-1}))$$

State

The state has to be more complex because the filter now estimates both the position and the attitude. Furthermore, because of asynchronousity, we have to store the last angular velocity, the last linear velocity, and the last time the linear velocity has been updated (to retrieve $\Delta t_v = t - t_a$ where t_a is the last time we had an update from the accelerometer).

$$\mathbf{x}_t = (\mathbf{p}_t, \mathbf{q}_t, \boldsymbol{\omega}_t, \mathbf{a}_t, t_a)$$

The structure of this filter and all of the filters presented thereafter is as follow:

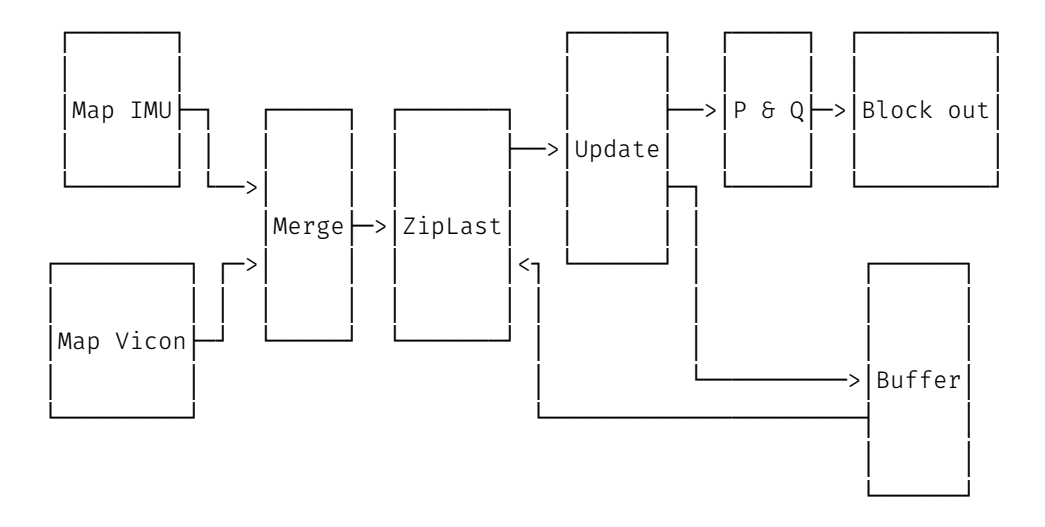


Figure 1.10: A graph of the filters structure in scala-flow

Kalman Filter

Bayesian inference

Bayesian inference is a method of statistical inference in which Bayes' theorem is used to update the probability for a hypothesis as more evidence or information becomes available. In this Bayes setting, the prior is the estimated distribution of the previous state at time t-1, the likelihood correspond to the likelihood of getting the new data from the sensor given the prior and finally, the posterior is the updated estimated distribution.

Model

The kalman filter requires that both the model process and the measurement process are **linear gaussian**. Linear gaussian processes are of the form:

$$\mathbf{x}_t = f(\mathbf{x}_{t-1}) + \mathbf{w}_t$$

where f is a linear function and \mathbf{w}_t a gaussian process: it is sampled from an arbitrary gaussian distribution.

The Kalman filter is a direct application of bayesian inference. It combines the prediction of the distribution given the estimated prior state and the state-transition model.

$$\mathbf{x}_t = \mathbf{F}_t \mathbf{x}_{t-1} + \mathbf{B}_t \mathbf{u}_t + \mathbf{w}_t$$

- \mathbf{x}_t the state
- \mathbf{F}_t the state transition model
- \mathbf{B}_t the control-input model
- \mathbf{u}_t the control vector
- \mathbf{w}_t process noise drawn from $\mathbf{w}_t \sim N(0, \mathbf{Q}_k)$

and the estimated distribution given the data coming from the sensors.

$$\mathbf{y}_t = \mathbf{H}_t \mathbf{x}_t + \mathbf{v}_t$$

- \mathbf{y}_t measurements
- \mathbf{H}_t the state to measurement matrix
- \mathbf{w}_t measurement noise drawn from $\mathbf{w}_t \sim N(0, \mathbf{R}_k)$

Because, both the model process and the sensor process are assumed to be linear gaussian, we can combine them into a gaussian distribution. Indeed, the product of two gaussians is gaussian.

$$P(\mathbf{x}_t) \propto P(\mathbf{x}_t^-|\mathbf{x}_{t-1}) \cdot P(\mathbf{x}_t|\mathbf{y}_t)$$
$$\mathcal{N}(\mathbf{x}_t) \propto \mathcal{N}(\mathbf{x}_t^-|\mathbf{x}_{t-1}) \cdot \mathcal{N}(\mathbf{x}_t|\mathbf{y}_t)$$

where \mathbf{x}_t^- is the predicted state from the previous state and the state-transition model.

The kalman filter keep track of the parameters of that gaussian: the mean state and the covariance of the state which represent the uncertainty about our last prediction. The mean of that distribution is also the best current state estimation of the filter.

By keeping track of the uncertainty, we can optimally combine the normals by knowing what importance to give to the difference between the expected sensor data and the actual sensor data. That factor is the Kalman gain.

- predict:
 - predicted state: $\hat{\mathbf{x}}_t^- = \mathbf{F}_t \mathbf{x}_{t-1} + \mathbf{B}_t \mathbf{u}_t$
 - predicted **covariance**: $\mathbf{\Sigma}_{t}^{-} = \mathbf{F}_{t-1}\mathbf{\Sigma}_{t-1}^{-}\mathbf{F}_{t-1}^{T} + \mathbf{Q}_{t}$
- update:
 - predicted **measurements**: $\hat{\mathbf{z}} = \mathbf{H}_t \hat{\mathbf{x}}_t^-$
 - innovation: $(\mathbf{z}_t \hat{\mathbf{z}})$
 - innovation covariance: $\mathbf{S} = \mathbf{H}_t \mathbf{\Sigma}_t^- \mathbf{H}_t^T + \mathbf{R}_t$
 - optimal kalman gain: $\mathbf{K} = \mathbf{\Sigma}_t^{-} \mathbf{H}_t^T \mathbf{S}^{-1}$
 - updated state: $\Sigma_t = \Sigma_t^- + KSK^T$
 - updated **covariance**: $\hat{\mathbf{x}}_t = \hat{\mathbf{x}}_t^- + \mathbf{K}(\mathbf{z}_t \hat{\mathbf{z}})$

Asynchronous Kalman Filter

It is not necessary to apply the full Kalman update at each measurement. Indeed, ${\bf H}$ can be sliced to correspond to the measurements currently available.

To be truly asynchronous, you also have to account for the different sampling rates. There is two cases :

- The required data for the update step (the control inputs) can arrive multiple time before any of the data of the update step (the measurements)
- Inversely, it is possible that the measurements occur at a higher sampling rate than the control inputs.

The strategy chosen here is as follows:

- 1. Multiple prediction steps without any update step may happen without making the algorithm inconsistent.
- 2. An update is **always** immediately preceded by a prediction step. This is a consequence of the requirement that the innovation must measure the difference between the predicted measurement from the state at the exact current time and the measurements. Thus, if the measurements are not synchronized with the control inputs, use the most likely control input for the prediction step. Repeating the last control input was the method used for the accelerometer and the gyroscope data as control input.

Extended Kalman Filters

In the previous section, we have shown that the Kalman Filter is only applicable when both the process model and the measurement model are linear Gaussian process.

- The noise of the measurements and of the state-transition must be Gaussian
- The state-transition function and the measurement to state function must be linear.

Furthermore, it is provable that Kalman filters are optimal linear filters.

However, in our context, one component of the state, the attitude, is intrinsically non-linear. Indeed, rotations and attitudes belong to SO(3) which is not a vector space. Therefore, we cannot use vanilla Kalman filters. The filters that we present thereafter relax those requirements.

One example of such extension is the extended Kalman filter (EKF) that we will present here. The EKF relax the linearity requirement by using differentiation to calculate an approximation of the first order of the required linear functions. Our state transition function and measurement function can now be expressed in the free forms $f(\mathbf{x}_t)$ and $h(\mathbf{x}_t)$ and we define the matrix \mathbf{F}_t and \mathbf{H}_t as their Jacobian.

$$\mathbf{F}_{t10\times10} = \left. \frac{\partial f}{\partial \mathbf{x}} \right|_{\hat{\mathbf{x}}_{t-1}, \mathbf{u}_{t-1}}$$

$$\mathbf{H}_{t7\times7} = \left. \frac{\partial h}{\partial \mathbf{x}} \right|_{\hat{\mathbf{x}}_t}$$

- predict:

 - predicted **state**: $\hat{\mathbf{x}}_t^- = f(\mathbf{x}_{t-1}) + \mathbf{B}_t \mathbf{u}_t$ predicted **covariance**: $\boldsymbol{\Sigma}_t^- = \mathbf{F}_{t-1} \boldsymbol{\Sigma}_{t-1}^- \mathbf{F}_{t-1}^T + \mathbf{Q}_t$
- update:
 - predicted **measurements**: $\hat{\mathbf{z}} = h(\hat{\mathbf{x}}_t^-)$
 - innovation: $(\mathbf{z}_t \hat{\mathbf{z}})$
 - innovation covariance: $\mathbf{S} = \mathbf{H}_t \mathbf{\Sigma}_t^- \mathbf{H}_t^T + \mathbf{R}_t$
 - optimal kalman gain: $\mathbf{K} = \mathbf{\Sigma}_t^{-} \mathbf{H}_t^{T} \mathbf{S}^{-1}$ updated state: $\mathbf{\Sigma}_t = \mathbf{\Sigma}_t^{-} + \mathbf{K} \mathbf{S} \mathbf{K}^{T}$

 - updated **covariance**: $\hat{\mathbf{x}}_t = \hat{\mathbf{x}}_t^- + \mathbf{K}(\mathbf{z}_t \hat{\mathbf{z}})$

EKF for POSE

State

For the EKF, we are gonna use the following state:

$$\mathbf{x}_t = (\mathbf{v}_t, \mathbf{p}_t, \mathbf{q}_t)^T$$

Initial state \mathbf{x}_0 at $(\mathbf{0}, \mathbf{0}, (1, 0, 0, 0))$

Indoor Measurements model

1. Position:

$$\mathbf{p}_{\mathbf{V}}(t) = \mathbf{p}(t)^{(i)} + \mathbf{p}_{\mathbf{V}_t^{\epsilon}}$$

where $\mathbf{p}_{\mathbf{V}_t}^{\epsilon} \sim \mathcal{N}(\mathbf{0}, \mathbf{R}_{\mathbf{p}_{\mathbf{V}_t}})$

2. Attitude:

$$\mathbf{q_V}(t) = \mathbf{q}(t)^{(i)}*R2Q(\mathbf{q_V}_t^\epsilon)$$
 where $\mathbf{q_V}_t^\epsilon \sim \mathcal{N}(\mathbf{0}, \mathbf{R_{q_{\mathbf{V}_t}}})$

Kalman prediction

The model dynamic defines the following model, state-transition function $f(\mathbf{x}, \mathbf{u})$ and process noise \mathbf{w} with covariance matrix \mathbf{Q}

$$\mathbf{x}_t = f(\mathbf{x}_{t-1}, \mathbf{u}_t) + \mathbf{w}_t$$

$$f((\mathbf{v}, \mathbf{p}, \mathbf{q}), (\mathbf{a}_{\mathbf{A}}, \boldsymbol{\omega}_{\mathbf{G}})) = \begin{pmatrix} \mathbf{v} + \Delta t \mathbf{R}_{b2f} \{ \mathbf{q}_{t-1} \} \mathbf{a} \\ \mathbf{p} + \Delta t \mathbf{v} \\ \mathbf{q} * R2Q(\Delta t \boldsymbol{\omega}_{G}) \end{pmatrix}$$

Now, we need to derive the jacobian of f. We will use sagemath to retrieve the 28 relevant different partial derivatives of q.

$$\mathbf{F}_{t10\times10} = \left. \frac{\partial f}{\partial \mathbf{x}} \right|_{\hat{\mathbf{x}}_{t-1}, \mathbf{u}_{t-1}}$$

$$\hat{\mathbf{x}}_t^{-(i)} = f(\mathbf{x}_{t-1}^{(i)}, \mathbf{u}_t)$$
$$\boldsymbol{\Sigma}_t^{-(i)} = \mathbf{F}_{t-1} \boldsymbol{\Sigma}_{t-1}^{-(i)} \mathbf{F}_{t-1}^T + \mathbf{Q}_t$$

Kalman measurements update

$$\mathbf{z}_t = h(\mathbf{x}_t) + \mathbf{v}_t$$

The measurement model defines $h(\mathbf{x})$

$$\left(\begin{array}{c} \mathbf{p}\mathbf{v} \\ \mathbf{q}\mathbf{v} \end{array}\right) = h((\mathbf{v}, \mathbf{p}, \mathbf{q})) = \left(\begin{array}{c} \mathbf{p} \\ \mathbf{q} \end{array}\right)$$

The only complex partial derivatives to calculate are the one of the acceleration, because they have to be rotated first. Once again, we use sagemath: $\mathbf{H_a}$ is defined by the script in the appendix B.

$$\begin{aligned} \mathbf{H}_{t10\times7} &= \left. \frac{\partial h}{\partial \mathbf{x}} \right|_{\hat{\mathbf{x}}_t} = \begin{pmatrix} \mathbf{0}_{3\times3} & & \\ & \mathbf{I}_{3\times3} & \\ & & \mathbf{I}_{4\times4} \end{pmatrix} \\ \mathbf{R}_{t7\times7} &= \begin{pmatrix} \mathbf{R}_{\mathbf{p}_{\mathbf{V}}} & & \\ & & \mathbf{R}'_{\mathbf{q}_{\mathbf{V}}4\times4} \end{pmatrix} \end{aligned}$$

 $\mathbf{R}'_{\mathbf{q_V}}$ has to be 4×4 and has to represent the covariance of the quaternion. However, the actual covariance matrix $\mathbf{R}_{\mathbf{q_V}}$ is 3×3 and represent the noise in terms of a *rotation vector* around the x, y, z axes.

We transform this rotation vector into a quaternion using our function R2Q. We can compute the new covariance matrix $\mathbf{R'_{q_V}}$ using Unscented Transform.

Unscented Transform

The unscented transform (UT) is a mathematical function used to estimate statistics after applying a given nonlinear transformation to a probability distribution. The idea is to use points that are representative of the original distribution, sigma points. We apply the transformation to those sigma points and calculate the new statistics using the transformed sigma points. The sigma points must have the same mean and covariance than the original distribution.

The minimal set of symmetric sigma points can be found using the covariance of the initial distribution. The 2N+1 minimal symmetric set of sigma points are the mean and the set of points corresponding to the mean plus and minus one of the direction corresponding to the covariance matrix. In one dimension, the square root of the variance is enough. In N-dimension, you must use the Cholesky decomposition of the covariance matrix. The Cholesky decomposition find the matrix L such that $\Sigma = LL^t$.

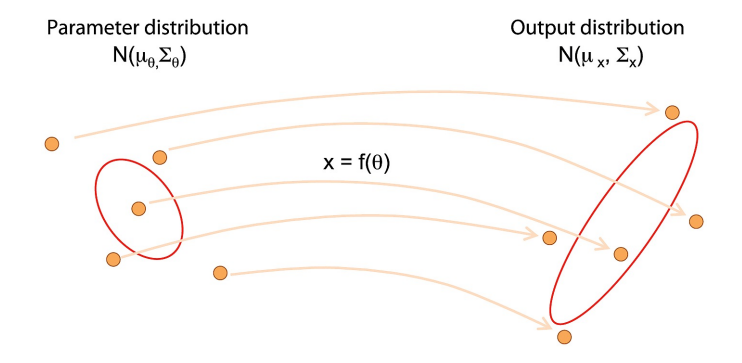


Figure 1.11: Unscented tranformation

Kalman update

$$\begin{split} \mathbf{S} &= \mathbf{H}_t \mathbf{\Sigma}_t^- \mathbf{H}_t^T + \mathbf{R}_t \\ \hat{\mathbf{z}} &= h(\hat{\mathbf{x}}_t^-) \\ \mathbf{K} &= \mathbf{\Sigma}_t^- \mathbf{H}_t^T \mathbf{S}^{-1} \\ \mathbf{\Sigma}_t &= \mathbf{\Sigma}_t^- + \mathbf{K} \mathbf{S} \mathbf{K}^T \\ \hat{\mathbf{x}}_t &= \hat{\mathbf{x}}_t^- + \mathbf{K} (\mathbf{z}_t - \hat{\mathbf{z}}) \end{split}$$

F partial derivatives

```
Q.<i,j,k> = QuaternionAlgebra(SR, -1, -1)
var('q0, q1, q2, q3')
var('dt')
var('wx, wy, wz')
q = q0 + q1*i + q2*j + q3*k
w = vector([wx, wy, wz])*dt
w_norm = sqrt(w[0]^2 + w[1]^2 + w[2]^2)
ang = w norm/2
w_normalized = w/w_norm
sin2 = sin(ang)
qd = cos(ang) + w_normalized[0]*sin2*i + w_normalized[1]*sin2*j
    + w normalized[2]*sin2*k
nq = q*qd
v = vector(nq.coefficient_tuple())
for sym in [wx, wy, wz, q0, q1, q2, q3]:
    d = diff(v, sym)
    exps = map(lambda x: x.canonicalize_radical().full_simplify(), d)
    for i, e in enumerate(exps):
        print(sym, i, e)
```

Unscented Kalman Filters

The EKF has 3 flaws in our case:

• The linearization gives an approximate form which result in approximation errors

- The prediction step of the EKF assume that the linearized form of the transformation can capture all the information needed to apply the transformation to the gaussian distribution pre-transformation. Unfortunately, this is only true near the region of the mean. The transformation of the tail of the gaussian distribution may need to be very different.
- It attempts to define a Gaussian covariance matrix for the attitude quaternion. This does not make sense because it does not account for the requirement of the quaternion being in a 4 dimensional unit sphere.

The Unscented Kalman Filter (UKF) does not suffer from the two first flaws, but it is more computationally expensive as it requires a Cholesky factorisation that grows exponentially in complexity with the number of dimensions.

Indeed, the UKF applies an unscented transformation to sigma points of the current approximated distribution. The statistics of the new approximated Gaussian are found through this unscented transform. The EKF linearizes the transformation, the UKF approximates the resulting Gaussian after the transformation. Hence, the UKF can take into account the effects of the transformation away from the mean which might be drastically different.

The implementation of an UKF still suffer greatly from quaternion not belonging to a vector space. The approach taken by [3] is to use the error quaternion defined by $\mathbf{e}_i = \mathbf{q}_i \bar{\mathbf{q}}$. This approach has the benefit that similar quaternion differences result in similar error. But apart from that, it does not have any profound justification. We must compute a sound average weighted quaternion of all sigma points. An algorithm is described in the following section.

Average quaternion

Unfortunately, the average of quaternions components $\frac{1}{N} \sum q_i$ or barycentric mean is unsound: Indeed, attitude do not belong to a vector space but a homogenous Riemannian manifold (the four dimensional unit sphere). To convince yourself of the unsoundness of the barycentric mean, see that the addition and barycentric mean of two unit quaternion is not necessarily an unit quaternion ((1,0,0,0) and (-1,0,0,0) for instance. Furthermore, angle being periodic, the barycentric mean of a quaternion with angle -178° and another with same body-axis and angle 180° gives 1° instead of the expected -179° .

To calculate the average quaternion, we use an algorithm which minimize a metric that correspond to the weighted attitude difference to the average, namely the weighted sum of the squared Frobenius norms of attitude matrix differences.

$$\bar{\mathbf{q}} = arg \min_{q \in \mathbb{S}^3} \sum w_i ||A(\mathbf{q}) - A(\mathbf{q}_i)||_F^2$$

where \mathbb{S}^3 denotes the unit sphere.

The attitude matrix $A(\mathbf{q})$ and its corresponding Frobenius norm have been described in the quaternion section.

Intuition

The intuition of keeping track of multiple representative of the distribution is exactly the approach taken by the particle filter. The particle filter has the advantage that the distribution is never transformed back to a gaussian so there is less assumption made about the noise and the transformation. It is only required to be able to calculate the expectation from a weighted set of particles.

Particle Filter

Particle filters are computationally expensive. This is the reason why their usage is not very popular currently for low-powered embedded systems like drones. However, they are used in Avionics for planes since the computational resources are less scarce and the precision crucial. Accelerating hardware could widen the usage of particle filters to embedded systems.

Particle filters are sequential monte carlo methods. Like all monte carlo method, they rely on repeated sampling for estimation of a distribution.

The particle filter itself a weighted particle representation of the posterior:

$$p(\mathbf{x}) = \sum w^{(i)} \delta(\mathbf{x} - \mathbf{x}^{(i)})$$

where δ is the dirac delta function. The dirac delta function is zero everywhere except at zero, with an integral of one over the entire real line. It represents here the ideal probability density of a particle.

Importance sampling

The weights are computed through importance sampling. With importance sampling, each particle does not represent equally the distribution. Importance sampling enables to use sampling from another distribution to estimate properties from the target distribution of interest. In most cases, it can be used to focus sampling on a specific region of the distribution. In our case, by choosing the right importance distribution (the dynamics of the model as

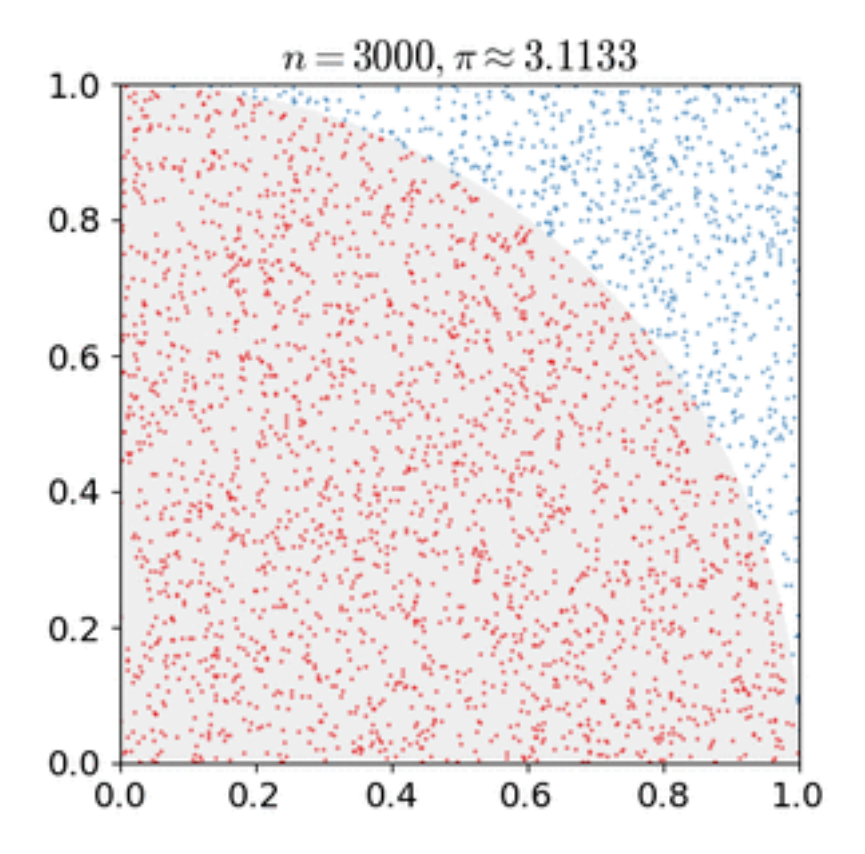


Figure 1.12: Monte Carlo estimation of pi

we will see later), we can reweight particles based on the likelihood from the measurements $(p(\mathbf{y}|\mathbf{x}))$.

Importance sampling is based on the identity:

$$\mathbb{E}[\mathbf{g}(\mathbf{x})|\mathbf{y}_{1:T}] = \int \mathbf{g}(\mathbf{x})p(\mathbf{x}|\mathbf{y}_{1:T})d\mathbf{x}$$
$$= \int \left[\mathbf{g}(\mathbf{x})\frac{p(\mathbf{x}|\mathbf{y}_{1:T})}{\pi(\mathbf{x}|\mathbf{y}_{1:T})}\right]\pi(\mathbf{x}|\mathbf{y}_{1:T})d\mathbf{x}$$

Thus, it can be approximated as

$$\mathbb{E}[\mathbf{g}(\mathbf{x})|\mathbf{y}_{1:T}] \approx \frac{1}{N} \sum_{i}^{N} \frac{p(\mathbf{x}^{(i)}|\mathbf{y}_{1:T})}{\pi(\mathbf{x}^{(i)}|\mathbf{y}_{1:T})} \mathbf{g}(\mathbf{x}^{(i)}) \approx \sum_{i}^{N} w^{(i)} \mathbf{g}(\mathbf{x}^{(i)})$$

where N samples of \mathbf{x} are drawn from the importance distribution $\pi(\mathbf{x}|\mathbf{y}_{1:T})$

And the weights are defined as:

$$w^{(i)} = \frac{1}{N} \frac{p(\mathbf{x}^{(i)}|\mathbf{y}_{1:T})}{\pi(\mathbf{x}^{(i)}|\mathbf{y}_{1:T})}$$

Computing $p(\mathbf{x}^{(i)}|\mathbf{y}_{1:T}$ is hard (if not impossible), but fortunately we can compute the unnormalized weight instead:

$$w^{(i)} * = p(\mathbf{y}_{1:T} | \mathbf{x}^{(i)}) p(\mathbf{x}^{(i)}) \pi(\mathbf{x}^{(i)} | \mathbf{y}_{1:T})$$

and normalizing it afterwards

$$\sum_{i}^{N} w^{(i)*} = 1 \Rightarrow w^{(i)} = \frac{w^{*(i)}}{\sum_{i}^{N} w^{*(i)}}$$

Sequential Importance Sampling

The last equation becomes more and more computationally expensive as T grows larger (the joint variable of the time series grows larger). Fortunately, Sequential Importance Sampling is an alternative recurisve algorithm that has a fixed amount of computation at each iteration:

$$p(\mathbf{x}_{0:k}|\mathbf{y}_{0:k}) \propto p(\mathbf{y}_k|\mathbf{x}_{0:k},\mathbf{y}_{1:k-1})p(\mathbf{x}_k|\mathbf{y}_{1:k-1})$$

$$\propto p(\mathbf{y}_k|\mathbf{x}_k)p(\mathbf{x}_k|\mathbf{x}_{0:k-1},\mathbf{y}_{1:k-1})p(\mathbf{x}_{0:k-1}|\mathbf{y}_{1:k-1})$$

$$\propto p(\mathbf{y}_k|\mathbf{x}_k)p(\mathbf{x}_k|\mathbf{x}_{k-1})p(\mathbf{x}_{0:k-1}|\mathbf{y}_{1:k-1})$$

The importance distribution is such that $\mathbf{x}_{0:k}^i \sim \pi(\mathbf{x}_{0:k}|\mathbf{y}_{1:k})$ with the according importance weight:

$$w_k^{(i)} \propto \frac{p(\mathbf{y}_k|\mathbf{x}_k^{(i)})p(\mathbf{x}_k^{(i)}|\mathbf{x}_{k-1}^{(i)})p(\mathbf{x}_{0:k-1}^{(i)}|\mathbf{y}_{1:k-1})}{\pi(\mathbf{x}_{0:k}|\mathbf{y}_{1:k})}$$

We can express the importance distribution recursively:

$$\pi(\mathbf{x}_{0:k}|\mathbf{y}_{1:k}) = \pi(\mathbf{x}_k|\mathbf{x}_{0:k-1},\mathbf{y}_{1:k})\pi(\mathbf{x}_{0:k-1}|\mathbf{y}_{1:k-1})$$

The recursive structure propagates to the weight itself:

$$w_k^{(i)} \propto \frac{p(\mathbf{y}_k|\mathbf{x}_k^{(i)})p(\mathbf{x}_k^{(i)}|\mathbf{x}_{k-1}^{(i)})}{\pi(\mathbf{x}_k|\mathbf{x}_{0:k-1},\mathbf{y}_{1:k})} \frac{p(\mathbf{x}_{0:k-1}^{(i)}|\mathbf{y}_{1:k-1})}{\pi(\mathbf{x}_{0:k-1}|\mathbf{y}_{1:k-1})}$$
$$\propto \frac{p(\mathbf{y}_k|\mathbf{x}_k^{(i)})p(\mathbf{x}_k^{(i)}|\mathbf{x}_{k-1}^{(i)})}{\pi(\mathbf{x}_k|\mathbf{x}_{0:k-1},\mathbf{y}_{1:k})} w_{k-1}^{(i)}$$

We can further simplify the formuly by choosing the importance distribution to be the dynamics of the model:

$$\pi(\mathbf{x}_k|\mathbf{x}_{0:k-1},\mathbf{y}_{1:k}) = p(\mathbf{x}_k^{(i)}|\mathbf{x}_{k-1}^{(i)})$$
$$w_k^{*(i)} = p(\mathbf{y}_k|\mathbf{x}_k^{(i)})w_{k-1}^{(i)}$$

As previously, it is then only needed to normalize the resulting weight.

$$\sum_{i}^{N} w^{(i)*} = 1 \Rightarrow w^{(i)} = \frac{w^{*(i)}}{\sum_{j}^{N} w^{*(i)}}$$

Resampling

When the number of effective particles is too low (less than 1/10 of N having weight 1/10), we apply systematic resampling. The idea behind resampling is simple. The distribution is represented by a number of particles with different weights. As time goes, the repartition of weights degenerate. A large subset of particles ends up having negligible weight which make them

irrelevant. In the most extreme case, one particle represents the whole distribution.

To avoid that degeneration, when the weights are too unbalanced, we resample from the weights distribution: pick N times among the particle and assign them a weight of 1/N, each pick has odd w_i to pick the particle p_i . Thus, some particles with large weights are splitted up into smaller clone particle and others with small weight are never picked. This process is similar to evolution, at each generation, the most promising branch survive and replicate while the less promising die off.

A popular method for resampling is systematic sampling as described by [4]:

Sample
$$U_1 \sim \mathcal{U}[0, \frac{1}{N}]$$
 and define $U_i = U_1 + \frac{i-1}{N}$ for $i = 2, \dots, N$

Rao-Blackwellized Particle Filter

Introduction

Compared to a plain particle filter, RPBF leverage the linearity of some components of the state by assuming our model gaussian conditionned on a latent variable: Given the attitude q_t , our model is linear. This is where RPBF shines: We use particle filtering to estimate our latent variable, the attitude, and we use the optimal kalman filter to estimate the state variable. If a plain particle can be seen as the simple average of particle states, then the RPBF can be seen as the "average" of many Gaussians. Each particle is an optimal kalman filter conditioned on the particle's latent variable, the attitude.

Indeed, the benefit of particle filters is that they assume no particular form for the posterior distribution and transformation of the state. But as the state widens in dimensions, the number of needed particles to keep a good estimation grows exponentially. This is a consequence of ["the curse of dimensionality"] (https://en.wikipedia.org/wiki/Curse_of_dimensionality): for each dimension, we would have to consider all additional combinations of state. In our context, we have 10 dimensions $(\mathbf{v}, \mathbf{p}, \mathbf{q})$ and it would be very computationally expensive to simulate a too large number of particles.

Kalman filters on the other hand do not suffer from such exponential growth, but as explained previously, they are inadequate for non-linear transformations. RPBF is the best of both world by combining a particle filter for the non-linear components of the state (the attitude) as a latent variable, and Kalman filters for the linear components of the state (velocity and position). For ease of notation, the linear component of the state will be referred to as the state and designated by \mathbf{x} even though the actual state we are concerned

with should include the latent variable θ .

Related work

Related work of this approach is [5]. However, it differs by:

- adapting the filter to drones by taking into account that the system is too
 dynamic for assuming that the accelerometer simply output the gravity
 vector. This is solved by augmenting the state with the acceleration as
 shown later.
- not using measurements of the IMU as control inputs (this is usually used for wheeled vehicles because of the drift from the wheels) but have both control inputs and measurements.
- add an attitude sensor.

Latent variable

We introduce the latent variable $\boldsymbol{\theta}$

The latent variable θ has for sole component the attitude:

$$\boldsymbol{\theta} = (\mathbf{q})$$

 q_t is estimated from the product of the attitude of all particles $\theta^{(i)} = \mathbf{q}_t^{(i)}$ as the "average" quaternion $\mathbf{q}_t = avgQuat(\mathbf{q}_t^n)$. x^n designates the product of all n arbitrary particle.

As stated in the previous section, The weight definition is:

$$w_t^{(i)} = \frac{p(\boldsymbol{\theta}_{0:t}^{(i)}|\mathbf{y}_{1:t})}{\pi(\boldsymbol{\theta}_{0:t}^{(i)}|\mathbf{y}_{1:t})}$$

From the definition and the previous section, it is provable that:

$$w_t^{(i)} \propto \frac{p(\mathbf{y}_t | \boldsymbol{\theta}_{0:t-1}^{(i)}, \mathbf{y}_{1:t-1}) p(\boldsymbol{\theta}_t^{(i)} | \boldsymbol{\theta}_{t-1}^{(i)})}{\pi(\boldsymbol{\theta}_t^{(i)} | \boldsymbol{\theta}_{1:t-1}^{(i)}, \mathbf{y}_{1:t})} w_{t-1}^{(i)}$$

We choose the dynamics of the model as the importance distribution:

$$\pi(\boldsymbol{\theta}_t^{(i)}|\boldsymbol{\theta}_{1:t-1}^{(i)},\mathbf{y}_{1:t}) = p(\boldsymbol{\theta}_t^{(i)}|\boldsymbol{\theta}_{t-1}^{(i)})$$

Hence,

$$w_t^{*(i)} \propto p(\mathbf{y}_t | \boldsymbol{\theta}_{0:t-1}^{(i)}, \mathbf{y}_{1:t-1}) w_{t-1}^{(i)}$$

We then sum all $w_t^{*(i)}$ to find the normalization constant and retrieve the actual $w_t^{(i)}$

State

$$\mathbf{x}_t = (\mathbf{v}_t, \mathbf{p}_t)^T$$

Initial state $\mathbf{x}_0 = (\mathbf{0}, \mathbf{0}, \mathbf{0})$

Initial covariance matrix $\Sigma_{6\times 6} = \epsilon \mathbf{I}_{6\times 6}$

Latent variable

$$\mathbf{q}_{t+1}^{(i)} = \mathbf{q}_t^{(i)} * R2Q(\Delta t(\boldsymbol{\omega}_{\mathbf{G}t} + \boldsymbol{\omega}_{\mathbf{G}_t}^{\epsilon}))$$

 $\omega_{\mathbf{G}_t^{\epsilon}}$ represents the error from the control input and is sampled from $\omega_{\mathbf{G}_t^{\epsilon}} \sim \mathcal{N}(\mathbf{0}, \mathbf{R}_{\omega_{\mathbf{G}_t}})$

Initial attitude $\mathbf{q_0}$ is sampled such that the drone pitch and roll are none (parallel to the ground) but the yaw is unknown and uniformly distributed.

Note that $\mathbf{q}(t+1)$ is known in the model dynamic because the model is conditioned under $\boldsymbol{\theta}_{t+1}^{(i)}.$

Indoor Measurement model

1. Position:

$$\mathbf{p}_{\mathbf{V}}(t) = \mathbf{p}(t)^{(i)} + \mathbf{p}_{\mathbf{V}_t^{\epsilon}}$$

where $\mathbf{p}_{\mathbf{V}_t^{\epsilon}} \sim \mathcal{N}(\mathbf{0}, \mathbf{R}_{\mathbf{p}_{\mathbf{V}_t}})$

2. Attitude:

$$\mathbf{q}_{\mathbf{V}}(t) = \mathbf{q}(t)^{(i)} * R2Q(\mathbf{q}_{\mathbf{V}_t^{\epsilon}})$$

where $\mathbf{q}_{\mathbf{V}_t^{\epsilon}} \sim \mathcal{N}(\mathbf{0}, \mathbf{R}_{\mathbf{q}_{\mathbf{V}_t}})$

Kalman prediction

The model dynamics define the following model, state-transition matrix $\mathbf{F}_t\{\boldsymbol{\theta}_t^{(i)}\}$, the control-input matrix $\mathbf{B}_t\{\boldsymbol{\theta}_t^{(i)}\}$, the process noise $\mathbf{w}_t\{\boldsymbol{\theta}_t^{(i)}\}$ for the Kalman filter and its covariance $\mathbf{Q}_t\{\boldsymbol{\theta}_t^{(i)}\}$

$$\begin{split} \mathbf{x}_t &= \mathbf{F}_t\{\boldsymbol{\theta}_t^{(i)}\}\mathbf{x}_{t-1} + \mathbf{B}_t\{\boldsymbol{\theta}_t^{(i)}\}\mathbf{u}_t + \mathbf{w}_t\{\boldsymbol{\theta}_t^{(i)}\} \\ &\mathbf{F}_t\{\boldsymbol{\theta}_t^{(i)}\}_{6\times 6} = \begin{pmatrix} \mathbf{I}_{3\times 3} & 0 \\ \Delta t \ \mathbf{I}_{3\times 3} & \mathbf{I}_{3\times 3} \end{pmatrix} \\ &\mathbf{B}_t\{\boldsymbol{\theta}_t^{(i)}\}_{6\times 3} = \begin{pmatrix} \mathbf{R}_{b2f}\{\mathbf{q}_t^{(i)}\}\mathbf{a}_{\mathbf{A}} \\ 0_{3\times 3} \end{pmatrix} \\ &\mathbf{Q}_t\{\boldsymbol{\theta}_t^{(i)}\}_{6\times 6} = \begin{pmatrix} \mathbf{R}_{b2f}\{\mathbf{q}_t^{(i)}\}(\mathbf{Q}_{\mathbf{a}_t} * dt^2)\mathbf{R}_{b2f}^t\{\mathbf{q}_t^{(i)}\} \\ &\mathbf{Q}_{\mathbf{v}_t} \end{pmatrix} \\ &\hat{\mathbf{x}}_t^{-(i)} &= \mathbf{F}_t\{\boldsymbol{\theta}_t^{(i)}\}\mathbf{x}_{t-1}^{(i)} + \mathbf{B}_t\{\boldsymbol{\theta}_t^{(i)}\}\mathbf{u}_t \\ &\mathbf{\Sigma}_t^{-(i)} &= \mathbf{F}_t\{\boldsymbol{\theta}_t^{(i)}\}\mathbf{\Sigma}_{t-1}^{-(i)}(\mathbf{F}_t\{\boldsymbol{\theta}_t^{(i)}\})^T + \mathbf{Q}_t\{\boldsymbol{\theta}_t^{(i)}\} \end{split}$$

Kalman measurement update

The measurement model defines how to compute $p(\mathbf{y}_t|\boldsymbol{\theta}_{0:t-1}^{(i)}, \mathbf{y}_{1:t-K1})$

Indeed, The measurement model defines the observation matrix $\mathbf{H}_t\{\boldsymbol{\theta}_t^{(i)}\}$, the observation noise $\mathbf{v}_t\{\boldsymbol{\theta}_t^{(i)}\}$ and its covariance matrix $\mathbf{R}_t\{\boldsymbol{\theta}_t^{(i)}\}$ for the Kalman filter.

$$(\mathbf{a}_{\mathbf{A}t}, \mathbf{p}_{\mathbf{V}t})^T = \mathbf{H}_t \{ \boldsymbol{\theta}_t^{(i)} \} (\mathbf{v}_t, \mathbf{p}_t)^T + \mathbf{v}_t \{ \boldsymbol{\theta}_t^{(i)} \}$$

$$\mathbf{H}_t \{ \boldsymbol{\theta}_t^{(i)} \}_{6 \times 3} = \begin{pmatrix} \mathbf{0}_{3 \times 3} & \\ & \mathbf{I}_{3 \times 3} \end{pmatrix}$$

$$\mathbf{R}_t \{ \boldsymbol{\theta}_t^{(i)} \}_{3 \times 3} = \begin{pmatrix} \mathbf{R}_{\mathbf{p}\mathbf{V}_t} \end{pmatrix}$$

Kalman update

$$\begin{split} \mathbf{S} &= \mathbf{H}_t \{\boldsymbol{\theta}_t^{(i)}\} \boldsymbol{\Sigma}_t^{-(i)} (\mathbf{H}_t \{\boldsymbol{\theta}_t^{(i)}\})^T + \mathbf{R}_t \{\boldsymbol{\theta}_t^{(i)}\} \\ \hat{\mathbf{z}} &= \mathbf{H}_t \{\boldsymbol{\theta}_t^{(i)}\} \hat{\mathbf{x}}_t^{-(i)} \\ \mathbf{K} &= \boldsymbol{\Sigma}_t^{-(i)} \mathbf{H}_t \{\boldsymbol{\theta}_t^{(i)}\}^T \mathbf{S}^{-1} \\ \boldsymbol{\Sigma}_t^{(i)} &= \boldsymbol{\Sigma}_t^{-(i)} + \mathbf{K} \mathbf{S} \mathbf{K}^T \\ \hat{\mathbf{x}}_t^{(i)} &= \hat{\mathbf{x}}_t^{-(i)} + \mathbf{K} ((\mathbf{a}_{\mathbf{A}t}, \mathbf{p}_{\mathbf{V}t})^T - \hat{\mathbf{z}}) \\ p(\mathbf{y}_t | \boldsymbol{\theta}_{0:t-1}^{(i)}, \mathbf{y}_{1:t-1}) &= \mathcal{N}((\mathbf{a}_{\mathbf{A}t}, \mathbf{p}_{\mathbf{V}t})^T; \hat{\mathbf{z}}_t, \mathbf{S}) \end{split}$$

Asynchronous measurements

Our measurements might have different sampling rate so instead of doing full kalman update, we only apply a partial kalman update corresponding to the current type of measurement \mathbf{z}_t .

For indoor, there is only one kind of sensor for the Kalman update: $\mathbf{P}\mathbf{v}$

Attitude re-weighting

In the measurement model, the attitude defines another re-weighting for importance sampling.

$$p(\mathbf{y}_t | \boldsymbol{\theta}_{0:t-1}^{(i)}, \mathbf{y}_{1:t-1}) = \mathcal{N}(Q2R(\mathbf{q^{(i)}}^{-1}\mathbf{q}_{\mathbf{V}_t}); 0, \mathbf{R}_{\mathbf{q}_{\mathbf{V}}})$$

Algorithm summary

- 1. Initiate N particles with \mathbf{x}_0 , $\mathbf{q}_0 \sim p(\mathbf{q}_0)$, Σ_0 and w = 1/N
- 2. While new sensor measurements $(\mathbf{z}_t, \mathbf{u}_t)$
- foreach N particles (i):
 - 1. Depending on the type of observation:
 - **IMU**:
 - 1. store $\omega_{\mathbf{G}_t}$ and $\mathbf{a}_{\mathbf{A}_t}$ as last control inputs
 - 2. sample new latent variable θ_t from ω_{G_t} (which correspond to the last control inputs)
 - 3. apply kalman prediction from $\mathbf{a}_{\mathbf{A}t}$ (which correspond to the last control inputs)

- Vicon:

- 1. sample new latent variable θ_t from $\omega_{\mathbf{G}t}$ (which correspond to the last control inputs)
- 2. apply kalman prediction from $\mathbf{a}_{\mathbf{A}t}$ (which correspond to the last control inputs)
- 3. Partial kalman update with:

$$\begin{aligned} \mathbf{H}_t \{\boldsymbol{\theta}_t^{(i)}\}_{3\times 6} &= (\mathbf{0}_{3\times 3} \quad \mathbf{I}_{3\times 3}) \\ \mathbf{R}_t \{\boldsymbol{\theta}_t^{(i)}\}_{3\times 3} &= \mathbf{R}_{\mathbf{p}_{\mathbf{V}_t}} \\ \mathbf{x}_t^{(i)} &= \mathbf{H}_t \{\boldsymbol{\theta}_t^{(i)}\} \mathbf{x}_{t-1}^{(i)} + \mathbf{K} (\mathbf{p}_{\mathbf{V}_t} - \hat{\mathbf{z}}) \\ p(\mathbf{y}_t | \boldsymbol{\theta}_{0:t-1}^{(i)}, \mathbf{y}_{1:t-1}) &= \mathcal{N} (\mathbf{q}_{\mathbf{V}_t}; \mathbf{q}_t^{(i)}, \ \mathbf{R}_{\mathbf{q}_{\mathbf{V}_t}}) \mathcal{N} (\mathbf{p}_{\mathbf{V}_t}; \hat{\mathbf{z}}_t, \mathbf{S}) \end{aligned}$$

- Other sensors (Outdoor): As for Vicon but use the corresponding partial Kalman update
- 2. Update $w_t^{(i)}$: $w_t^{(i)} = p(\mathbf{y}_t | \boldsymbol{\theta}_{0:t-1}^{(i)}, \mathbf{y}_{1:t-1}) w_{t-1}^{(i)}$
- Normalize all $w^{(i)}$ by scalaing by $1/(\sum w^{(i)})$ such that $\sum w^{(i)} = 1$
- Compute \mathbf{p}_t and \mathbf{q}_t as the expectation from the distribution approximated by the N particles.
- Resample if the number of effective particle is too low

Extension to outdoors

As highlighted in the Algorithm summary, the RPBF if easily extensible to other sensors. Indeed, measurements are either:

- giving information about position or velocity and their update is similar to the vicon position update as a kalman partial update
- giving information about the orientation and their update is similar to the vicon attitude update as a pure importance sampling re-weighting.

As a proof-of-conceptalternative Rao-blackwellized particle filter specialized for outdoor has been developed that integrates the following sensors:

- IMU with accelerometer, gyroscope and magnetometer
- Altimeter
- Dual GPS (2 GPS)
- Optical Flow

The optical flow measurements are assumed to be of the form $(\Delta \mathbf{p}, \Delta \mathbf{q})$ for a Δt corresponding to its sampling rate. It is inputed to the particle filter as a likelihood:

$$p(\mathbf{y}_t|\boldsymbol{\theta}_{0:t-1}^{(i)}, \mathbf{y}_{1:t-1}) = \mathcal{N}(\mathbf{p}_{t1} + \Delta p; \mathbf{p}_{t2}; \mathbf{R}_{\mathbf{d}\mathbf{p}_{\mathbf{O}_t}}) \mathcal{N}(\Delta \mathbf{q}; \mathbf{q}_{t1}^{-1} \mathbf{q}_{t2}; \mathbf{R}_{\mathbf{d}\mathbf{q}_{\mathbf{O}_t}})$$

where $t2 = t1 + \Delta t$, \mathbf{p}_{t2} is the latest kalman prediction and \mathbf{q}_{t2} is the latest latent variable through sampling of the attitude updates.

Results

We present a comparison of the 4 filters in 6 settings. The metrics is the RMSE of the 12-norm of the position and of the Froebius norm of the attitude as described previously. All the filters share a sampling frequency of 200Hz for the IMU and 4Hz for the Vicon. The RBPF is set to 1000 particles

In all scenarios, the covariance matrices of the sensors' measurements are diagonal:

- $$\begin{split} \bullet \quad & \mathbf{R_{a_A}} = \sigma_{\mathbf{a_A}}^2 \mathbf{I_{3\times 3}} \\ \bullet \quad & \mathbf{R_{\omega_G}} = \sigma_{\omega_G}^2 \mathbf{I_{3\times 3}} \\ \bullet \quad & \mathbf{R_{p_V}} = \sigma_{\mathbf{p_V}}^2 \mathbf{I_{3\times 3}} \\ \bullet \quad & \mathbf{R_{q_V}} = \sigma_{\mathbf{q_V}}^2 \mathbf{I_{3\times 3}} \end{split}$$

with the following settings:

• Vicon:

- $\begin{array}{l} \text{ High-precision } \sigma_{\mathbf{p_{V}}}^2 = \sigma_{\mathbf{q_{V}}}^2 = 0.01 \\ \text{ Low-precision } \sigma_{\mathbf{p_{V}}}^2 = \sigma_{\mathbf{q_{V}}}^2 = 0.1 \end{array}$
- Accelerometer:
 - High-precision: $\sigma_{\mathbf{a_A}}^2 = 0.1$ Low-precision: $\sigma_{\mathbf{a_A}}^2 = 1.0$
- Gyroscope:
 - High-precision: $\sigma_{\omega_{\mathbf{G}}}^2 = 0.1$ Low-precision: $\sigma_{\omega_{\mathbf{G}}}^2 = 1.0$

Table 1.1: position RMSE over 5 random trajectories of 20 seconds

			Augmented			Rao -
Vicon			Complemen-	Extended	Unscented	Blackwellized
preci	Accel.	Gyros.	tary	Kalman	Kalman	Particle
sion	preci.	preci.	Filter	Filter	Filter	Filter
High	High	High	6.88e-02	3.26e-02	3.45e-02	1.45e-02
High	High	Low	6.10e-02	1.13e-01	9.20 e-02	2.17e-02
High	Low	Low	4.05e-02	5.24 e-02	3.29e-02	1.61e-02
Low	High	High	5.05e-01	5.05e-01	2.90e-01	1.27 e-01
Low	High	Low	6.16e-01	1.09e+00	9.30e-01	1.22e-01
Low	Low	Low	3.57e-01	2.66e-01	3.27e-01	1.19e-01

Table 1.2: attitude RMSE over 5 random trajectories of 20 seconds

			Augmented			Rao -
Vicon			Complemen-	Extended	Unscented	Blackwellized
preci	Accel.	Gyros.	tary	Kalman	Kalman	Particle
sion	preci.	preci.	Filter	Filter	Filter	Filter
High	High	High	7.36e-03	5.86e-03	5.17e-03	1.01e-04
High	High	Low	6.37e-03	1.37e-02	9.17e-03	$6.50 \mathrm{e}\text{-}04$
High	Low	Low	6.25 e-03	1.69 e-02	1.02e-02	$8.34\mathrm{e}\text{-}04$
Low	High	High	5.30e-01	3.28e-01	3.26e-01	5.82e-03
Low	High	Low	5.18e-01	2.99e-01	2.95e-01	5.78e-03
Low	Low	Low	5.90e-01	3.28e-01	3.24 e-01	3.97e-03

Figure 1.13 is a bar plot of the first line of each table.

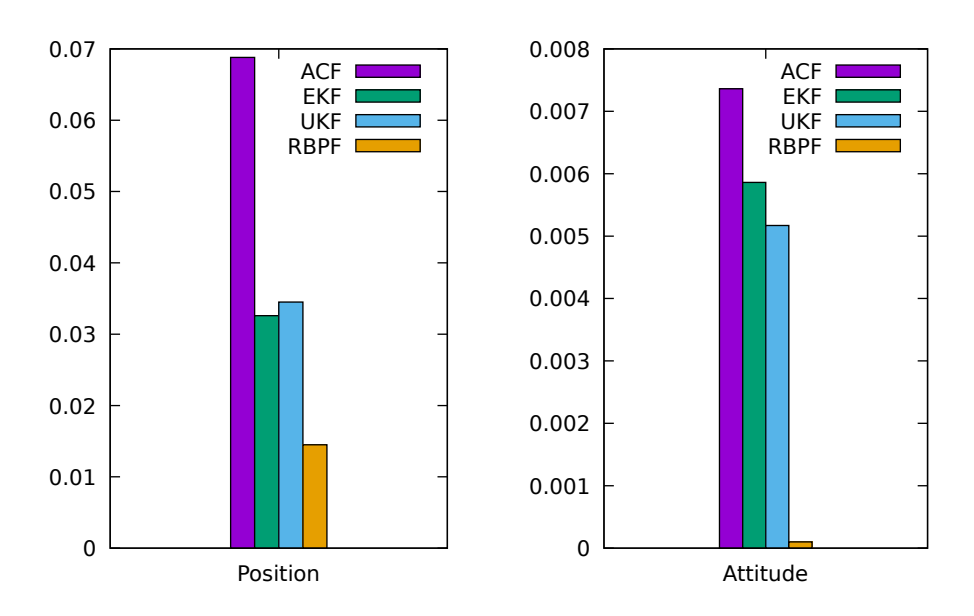


Figure 1.13: Bar plot in the High/High/High setting

Figure 1.14 is the plot of the tracking of the position (x, y, z) and attitute (r, i, j, k) in the **low** vicon precision, **low** accelerometer precision and **low** gyroscope precision setting for one of random trajectory.

Conclusion

The Rao-Blackwellized Particle Filter developed is more accurate than the alternatives, mathematically sound and computationally feasible. When implemented on hardware, this filter can be executed in real time with sensors of high and asynchronous sampling rate. It could improve POSE estimation

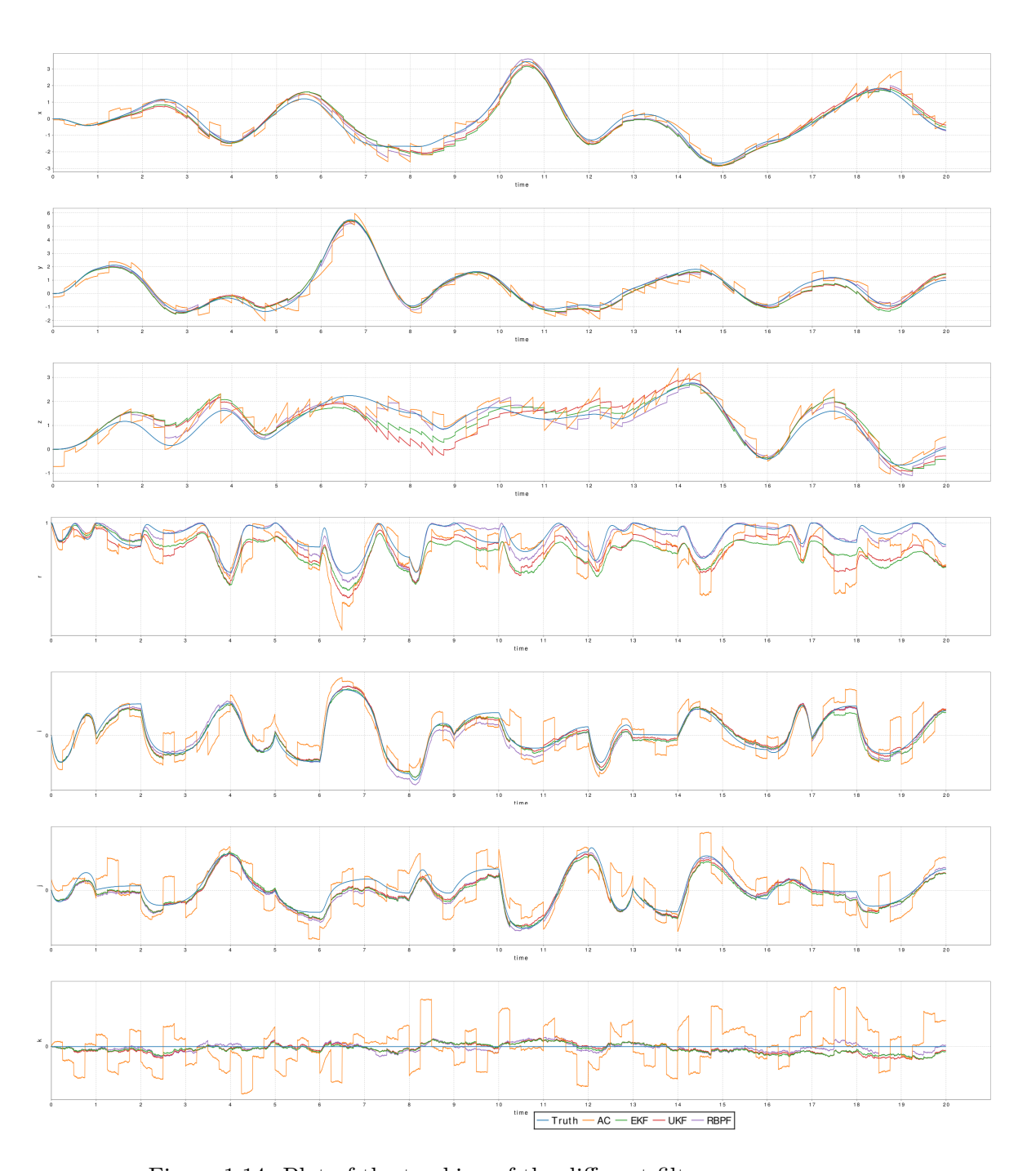


Figure 1.14: Plot of the tracking of the different filters

for all the existing drone and other robots. These improvements could unlock new abilities, potentials and increase the safeness of drone.

2 | A simulation tool for data flows with spatial integration: scala-flow

Purpose

Data flows are intuitive visual representation and abstraction of computations. As all forms of representations and abstractions, they help manage complexity, and let engineers reason on a higher level. They are common in the context of embedded systems, and most forms of data processing, in particular those related to the so called *big data*.

Spark and Simulink are popular libraries for data processing and embedded systems respectively. Spark grew popular as an alternative to Hadoop. The advantages of Spark over Hadoop was, among others, in-memory communication between nodes (as opposite of through file) and a functionnally inspired scala api that brought better abstractions and greatly reduced the number of line of code.

Simulink by MathWorks on the other hand, is a graphical programming environment for modeling, simulating and analyzing dynamic systems including potentially embedded systems. Its primary interface is a graphical block diagramming tool and a customizable set of block libraries.

scala-flow is inspired by both of these tools. It is general purpose in the sense that it can be used to represent any dynamic systems. Nevertheless, its primary intended usage is to develop, prototype, and debug embedded systems that use hardware reprogrammed by spatial. scala-flow has a functional/composable api, displays the constructed graph, provide block constructions. It provides some strong type safety: the type of the input and output of each node is checked at compilation to ensure the soundness of the resulting graph.

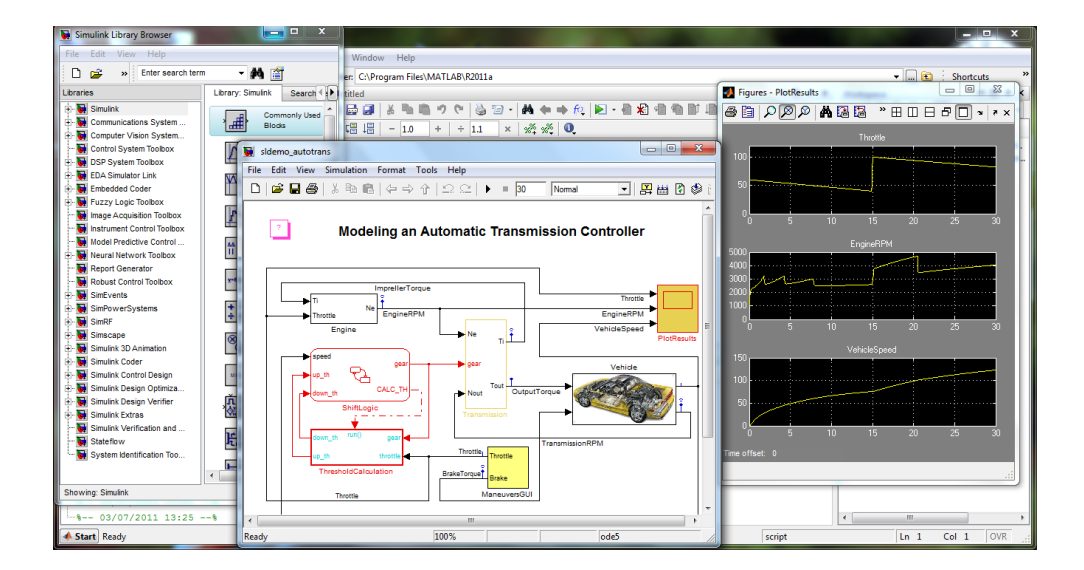


Figure 2.1: An example of the simulink interface

Source, Sink and Transformations

Data is under the form of "packets" containing a value of arbitrary type, an emission timestamp and the delays the packet has encountered through the different node processing.

```
case class Timestamped[A](t: Time, v: A, dt: Time)
```

(They are called Timestamped because they represent the value with timestamp informations.)

Data get emitted from sources (nodes with no input), processed and tranformed by other nodes until they reach sinks (nodes with no output). The nodes are connected between each other in many forms.

Nodes all mix-in the common trait Node. Every nodes also mix-in the trait Source[A] whose type parameter A indicates the type parameters of the packets emitted by this node. Indeed, nodes can only have one output. Every nodes also minx-in the trait SourceX[A, B, ...] where X is the arity of the number of input for that nodes and replace by the actual arity (1, 2, 3, ...). This is similar to FunctionX which is the type of functions in scala.

- SourceO indicates that the node takes exactly O input.
- Source1[A] indicates that the node has 1 input whose packets are of type A.
- Source2[A,B] indicates that the nodes has 2 inputs whose packets are respectively of type A and B
- etc ...

Since all nodes mix-in a SourceX, the compiler can check that the

inputs of each node are of the right type.

All SourceX must define def listenI(x: A) where I goes from 1 to X and A correspond to the corresponding type parameter of SourceX. def listenI(x: A) defines the action to take whenever a packet is received from the input I. In most cases, it is a transformation of x followed by a broadcasting (with the function def broadcast(x: R)) to the nodes that have for source this node.

There is a special case, SourceN[A, R] which represent nodes that have -arity of type A and emit packets of type R. For instance, the Plot nodes take number of sources and display them all on the same plot. The only constraint is that all the source nodes must emit the same kind of data of type A. Else it would not make sense to compare them. For plot specifically, A has also a view bound of Data which means that there exists a conversion from A to a Seq[Float], to ensure that A is displayable in a multiplot as timeseries. The x-axis, the time, correspond to the timestamp of emission contained in the packet.

An intermediary node that applies a transformation mixs-in the trait OpX[A, B, ..., R] where A, B is the type of the input, and R is the type of the output. Indeed,

```
OpX[A, B, ..., R] extends SourceX[A, B, ...] with Source[R].

For instance zip(sourceA, sourceB) is an Op[A, B, (A, B)]
```

Demo

Below is the scala-flow code corresponding to a data-flow that enable to compare a particle filter, an extended kalman filter, and the true state of the underlying model. At each tick of the different clocks, a packet containing the time as value is sent to nodes representing sensors. Those sensors have access to the model that is not represented here (the trajectory of the drone) and transform the time into noisy sensor measurements and forward them to the two filters. The packets once processed by the filters are plotted by the Plot sink. The plot also take as input the true state as given by the "toPoints" transformation.

```
//***** Model *****
val dtIMU = 0.01
val dtVicon = (dtIMU * 5)

val covAcc = 1.0
val covGyro = 1.0
val covViconP = 0.1
val covViconQ = 0.1
val numberParticles = 1200
```

```
val clockIMU = new TrajectoryClock(dtIMU)
val clockVicon = new TrajectoryClock(dtVicon)
val imu = clockIMU.map(IMU(eye(3) * covAcc, eye(3) * covGyro, dtIMU))
val vicon = clockVicon.map(Vicon(eye(3) * covViconP, eye(3) * covViconQ))
lazy val pfilter =
   ParticleFilterVicon(
     imu,
      vicon,
     numberParticles,
     covAcc,
     covGyro,
     covViconP,
     covViconQ
lazy val ekfilter =
    EKFVicon(
     imu,
     vicon,
     covAcc,
     covGyro,
     covViconP,
     covViconQ
val filters = List(ekfilter, pfilter)
val points = clockIMU.map(LambdaWithModel(
  (t: Time, traj: Trajectory) ⇒ traj.getPoint(t)), "toPoints")
val pqs = points.map(x \Rightarrow (x.p, x.q), "toPandQ")
Plot(pqs, filters:_*)
```

Figure 2.2: scala-flow program

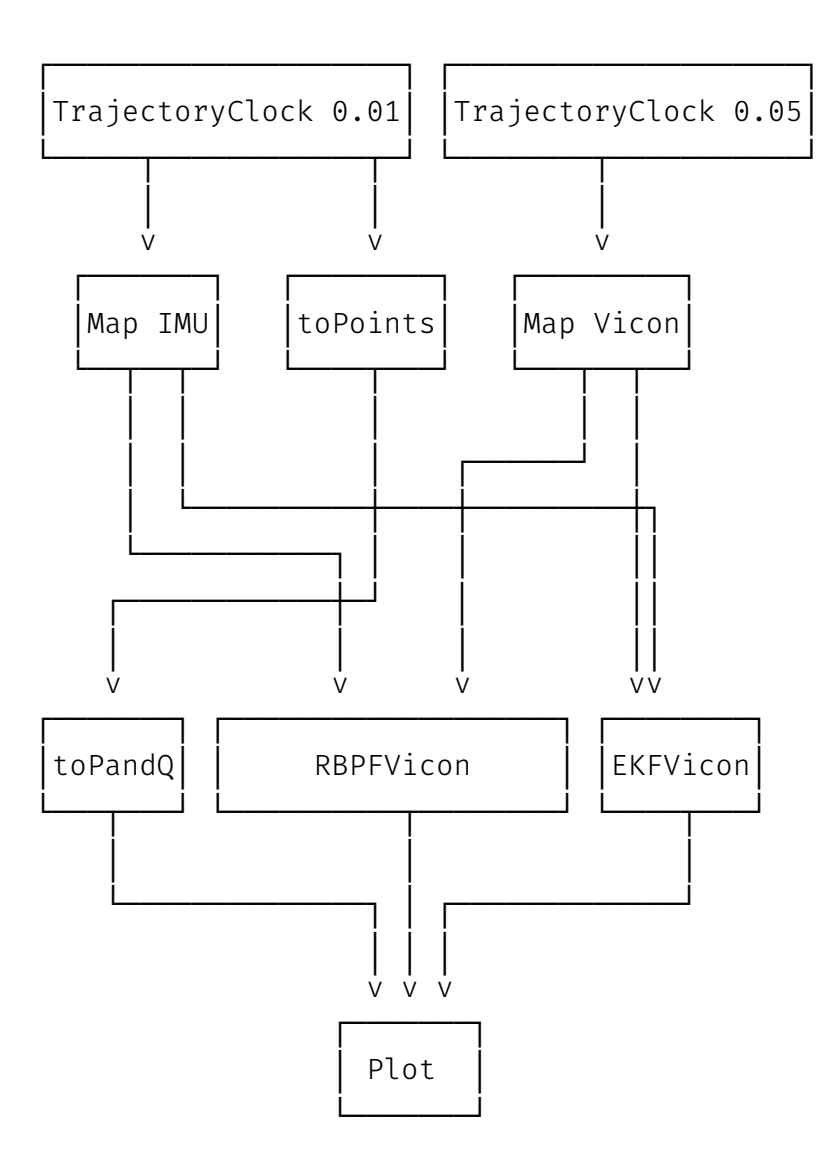


Figure 2.3: Graph representation of the data-flow

Block

A block is a node that actually represents a group of node. That node can be summarized by its input and output such that from an outside perspective, it can be considered as a simple node. Similar to the way an interface or an API hide its implementation details, a block hides its inner workings to the rest of the data-flow as long as the block process and emit the right type of packet. This logic extend to the graphical representation. Blocks are represented as nodes in the high-level graph but expanded in an independent graph below.

Similar to OpX[A, B, ..., R], there exists BlockX[A, B, ..., R]

which all extend Block[R] and take X sources as input. All Block[R] must define an out method of the form: def out: Source[R].

The filters are block with the following signatures:

Figure 2.4: Signature of the block of the particle filter

and similar for EKFVicon.

The observant reader might notice that the above block take as arguments rawSource and not Source directly. However, the packets are incoming from Source (def imu = source1). This is a consequence of intermediary Source potentially needing to be generated during the graph creation to synchronize multiple scheduler together.

Buffer and cycles

Source API

Here is a simplified description of the API of each source.

When relevant, the functions have an alternative methodNameT function that takes themselves function whose domain is Timestamped[A] instead of A.

For instance, there is a

```
def foreachT(f: Timestamped[A] ⇒ Unit): Source[A]
```

that is equivalent to the foreach below except it can access the additional fields in Timestamped

```
trait Source[A] {
  /** return a new source that map every incoming packet by the function f
   * such that new packets are Timestamped[B]
  def map[B](f: A \Rightarrow B): Source[B]
  /** return a filtered source that only broadcast
   * the elements that satisfy the predicate b */
  def filter(b: A ⇒ Boolean): Source[A]
  /** return this source and apply the function f to each
   * incoming packets as soon as they are received
  def foreach(f: A ⇒ Unit): Source[A]
  /** return a new source that broadcast elements
   * until the first time the predicate b is not satisfied
  def takeWhile(b: A ⇒ Boolean): Source[A]
  /** return a new source that accumulate As into a List[A]
    * then broadcast it when the next packet from the other
    * source clock is received
  def accumulate(clock: Source[Time]): Source[ListT[A]]
  /** return a new source that broadcast all element inside the collection
   * returned by the application of f to all incoming packet
  def flatMap[C](f: A ⇒ List[C]): Source[C]
  /** assumes that A is a List[Timestamped[B]].
   * returns a new source that apply the reduce function
    * over the collection contained in every incoming packet */
  def reduce[B](default: B, f: (B, B) \Rightarrow B)
      (implicit ev: A <:< ListT[B]): Source[B]</pre>
  /** return a new source that broadcast pair of the packet from this source
   * and the source provided as argument. Wait until a packet is received
    \star from both source. Packets from both source are queued such
   * that independant of the order, they are never discarded 
* A2 B1 A3 B2 B3 B4 B5 A4\Rightarrow (A1, B1), (A2, B2), (A3, B3), (A4, B4),
    * [Queue[B5]]
  def zip[B](s2: Source[B]): Source[Boolean]
  /** return a new source that broadcast pair of the packet from this source
   * and the source provided as argument. Similar to zip except that
    * if multiple packets from the source provided as argument is received
   * before, all except the last get discarded.
    * A2 B1 A3 B2 B3 B4 B5 A4\Rightarrow (A1, B1), (A2, B2), (A3, B3), (A4, B4),
   * [Queue[B5]]
   */
  def zipLastRight[B](s2: Source[B])
  /** return a new source that broadcast pair of the packet from this source
   * and the source provided as argument. Similar to zip except that all
   * packet except the last get discarded when both source are not in sync. 
 * A1 A2 B1 A3 B2 B3 A4\Rightarrow (A1, B1), (A3, B2), (B3, A4)
  def zipLast[B](s2: Source[B])
  /** return a new source that combine this source and the provided source .
  * packets from this source are Left
```

```
* packets from the other source are Right
  def merge[B](s2: Source[B]): Source[Either[A, B]]
  /** return a new source that fuse this source and the provided source
   * as long they have the same type.
    * any outgoing packet is indistinguishable of origin
  def fusion(sources: Source[A]*): Source[A]
 /** "label" every packet by the group returned by f */ def groupBy[B](f: A \Rightarrow B): Source[(B, A)]
  /** print every incoming packet */
  def debug(): Source[A]
  /** return a new source that buffer 1 element and
   * broadcast the buffered element with the time of the incoming A
  def bufferWithTime(init: A): Source[A]
  /** return a new source that do NOT broadcast any element */
  def muted: Source[A]
  /** return a new source that broadcast one incoming packet every
   * n incoming packet.
     The first broadcasted packet is the nth received one
   */
  def divider(n: Int): Source[A]
  /** return a pair of source from a source of pair */
  def unzip2[B, C](implicit ev: A <:< (B, C)): (Source[B], Source[C])</pre>
  /** return a new source whose every outgoing packet have an added dt
   * in their delay component
  def latency(dt: Time): Source[A]
  /** return a new source whose broadcasted packets contain the time of
    * emission
   */
  def toTime: Source[Time]
  /** return a new source that do NOT broadcast the first n packets */
 def drop(n: Int): Source[A]
implicit class TimeSource(source: Source[Time]) {
  /** stop the broadcasting after the timeframe tf has elapsed */
  def stop(tf: Timeframe): Source[Time]
  /** add a random delay following a gaussian with corresponding
   * mean and variance */
  def latencyVariance(mean: Real, variance: Real): Source[Time]
  /** add a delay of dt */
  def latency(dt: Time): Source[Time]
  /** return a new source of the difference of time between
   * the two last emitted packets */
  def deltaTime(init: Time = 0.0): Source[Time]
}
```

Figure 2.5: API of the Sources

The real API includes also a name and silent parameter. Both are only relevant for the graphical representation. The name of the block will be overriden by name if present and the node will be skipped in the graphical representation if silent is present.

Batch

A batch is a node that process its input in "batch" mode. All the other nodes process their input in "stream" mode. By "stream" mode, we mean that the node is able to process the input one-by-one, as soon as it arrives. The "batch" mode means that the node can only process i

Scheduling

Scheduling is the core mechanism of scala-flow. Scheduling ensure that packets gets emitted by the sending nodes and received by the recipient nodes at the "right time". Since scala-flow is a simulation tool, the "scala-flow time" does not correspond at all to the real time. Scheduling emits the packets as fast as it can. Therefore, since time is an arbitrary component of the packet, the only constraint that scheduling must satisfy is emitting the packets from all nodes in the right order.

Scheduling is achieved by one or many Schedulers. Schedulers are essentially queue of actions. The actions are side-effect functions that emit packets to the right node by the intermediary of channels. In the trivial case where there is no Batch, only one scheduler is needed.

Replay

Graph construction

InitHook

ModelHook

NodeHook

To gather the nodes and their connection between each other, a NodeHook is used. Every node must have access to a NodeHook to add itself to the registry. For the nodes that take no input, the SourceO, the NodeHook is passed as an implicit parameter. For the following nodes, the NodeHook is propagated since all others nodes use as NodeHook the one from their source1. This is similar to the way Scheduler are propagated through the graph.

Graphical representation

The graphical representation is in the ASCII format. The library asciigraphs is used to generate the output in ASCII from sets of vertices and edges. The set of vertices and edges is retrieved from the set of nodes contained in NodeHook.

FlowApp

A FlowApp[A, B] is an extension of the scala App. Its type parameters correspond to the type parameter of the InitHook and ModelHook

Channel

A single FlowApp can be run multiple times

Spatial integration

Conclusion

TODO

3 An interpreter for spatial

Spatial: An Hardware Description Language

Building applications is only made possible thanks to the many layers of abstractions that start fundamentally at the level of electrons. It is easy to forget how much of an exceptional feat of engineering.

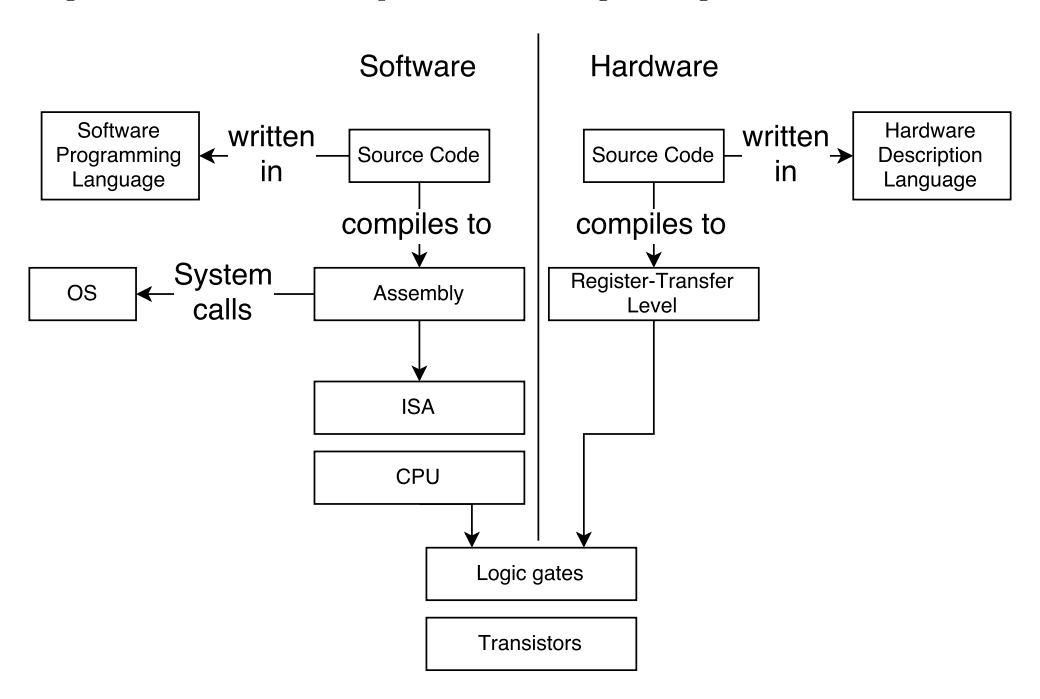


Figure 3.1: An Hardware vs Software abstraction layers overview

An Hardware Description Language (HDL) is used to describe the circuits on which applications runs on. A Software programming language is used to describe the applications themselves. Fundamentally, their purpose is different. But with a sufficient level of abstraction, they share many similarities.

c := a + b would translate in software by an instruction to store in

the memory (stack or heap) the sum of a and b stored themselves somewhere in memory. In hardware, depending on whether C represents a wire, a register, a memory location in SRAM or DRAM, the circuit is changed. However, from the user perspective, the source code is the same. One could think that it would be possible to write Hardware the same way than Software, but it is delusional. Some concepts are tied to the intrinsic nature of Hardware and inexpressible in the world of Software. A DSL that would abstract away those differences would result in a great loss of control for the user. Nevertheless, with the right level of abstraction it is possible to at least bridge the gap to a level satisfying for both the Software and Hardware engineers. This is the motivation behind Spatial.

Spatial is an (HDL) born out of the difficulties and complexity of doing Hardware. An HDL compiles to RTL which is equivalent to assembly in the software world and then the RTL is synthesized as Hardware (either as ASIC or as a bitstream reconfiguration data). The current alternatives available are Verilog, VHDL, Chisel and many others. What set apart Spatial from the crowd is that Spatial has a higher level of abstraction by leveraging parallel patterns and abstracting control flows as language constructs. Parallel patterns and control flows are detailed in Part IV.

Argon

Spatial is built on top of Argon, a fork of Lightweight Modular Staging (LMS). Argon and LMS are scala libraries that enable staged programming (or also called staged meta-programming). Argon lets user write meta-programs that are programs generators: programs that generate other programs.

Using Argon, language designer can specify a domain specific language and write their custom compiler for it. - **two-staged**: - **heterogenous**: The

TODO

Simulation in Spatial

Benefits of the interpreter

Building an interpreter for Spatial was a requirement for having a spatial integration in scala-flow. But it also benefits the whole spatial ecosystem. Indeed, an interpreter encourage the user to have more interactions with the language.

${\bf Interpreter}$

4 | Spatial implementation of an asynchronous Rao-Blackwellized Particle Filter

Parallel patterns

Parallel patterns

TODO

Controls flows

Control flows (or flow of control) is the order in which individual statements, instructions or function calls of an imperative program are executed or evaluated. Sequential Parallel Pipeline: Inner Pipe: Basic form of pipelining; Pipelining of primitive instructions. Coarse-Grain: Pipelining of parralel patterns Stream Pipe: ASAP with FIFOs stack or Streams: Stream(*)

TODO

A matrix library as stdlib

Mini Particle Filter

Rao Blackwellized Particle Filter

Conclusion

alea jacta est

Acknowledgments

Thank you to my parents for their continuous support, to Prof. Kunle and Prof. Odersky for supervising me and giving me the opportunity of doing this master thesis in their lab, to the entire lab of DAWN, in particular David Koeplinger, Raghu Prabhakar, Matt Feldman, Yaqi Zhang, Tian Zhao, Stefan Hadjis which accepted me as their peer for the length of my stay. I would also like to thank Nada Amin which supervised me in the semester project that led to this project and accepted to be an expert for the evaluation of the thesis. I am also grateful to the whole institution of EPFL for the education I have received those last 5 years and for which this thesis represents the culmination. Finally, to Stanford for having welcomed me for 6 months as a Visiting Researcher Student.

References

- [1] M. W. Mueller, M. Hehn, and R. D'Andrea, "A computationally efficient motion primitive for quadrocopter trajectory generation," *IEEE Transactions on Robotics*, vol. 31, no. 6, pp. 1294–1310, 2015.
- [2] F. L. Markley, Y. Cheng, J. L. Crassidis, and Y. Oshman, "Averaging quaternions," *Journal of Guidance, Control, and Dynamics*, vol. 30, no. 4, pp. 1193–1197, 2007.
- [3] K. Edgar, "A Quaternion-based Unscented Kalman Filter for Orientation Tracking.".
- [4] A. Doucet and A. M. Johansen, "A tutorial on particle filtering and smoothing: Fifteen years later," *Handbook of nonlinear filtering*, vol. 12, nos. 656-704, p. 3, 2009.
- [5] P. Vernaza and D. D. Lee, "Rao-Blackwellized particle filtering for 6-DOF estimation of attitude and position via GPS and inertial sensors," in *Robotics and Automation*, 2006. ICRA 2006. Proceedings 2006 IEEE International Conference on, 2006, pp. 1571–1578.